

Sgoldstino-Higgs mixing in models with low-scale supersymmetry breaking

K. O. Astapov^{a,b,1}, S. V. Demidov^{a,b,2}

^a*Institute for Nuclear Research of the Russian Academy of Sciences,
60th October Anniversary prospect 7a, Moscow 117312, Russia*

^b*Department of Particle Physics and Cosmology, Physics Faculty,
M. V. Lomonosov Moscow State University,
Vorobjevy Gory, 119991, Moscow, Russia*

Abstract

We consider a supersymmetric extension of the Standard Model with low-scale supersymmetry breaking. Besides usual superpartners it contains additional chiral goldstino supermultiplet whose scalar components – sgoldstinos – can mix with scalars from the Higgs sector of the model. We show that this mixing can have considerable impact on phenomenology of the lightest Higgs boson and scalar sgoldstino. In particular, the latter can be a good candidate for explanation of 2σ LEP excess with mass around 98 GeV.

PACS numbers:

¹**e-mail:** astapov@ms2.inr.ac.ru

²**e-mail:** demidov@ms2.inr.ac.ru

1 Introduction

Discovery of a new scalar resonance at the ATLAS [1] and CMS [2] becomes one of the most pronounced events in the last few years. During the 1st run of the LHC experiments in 2011-2012 there was collected statistics about 5 fb at $\sqrt{s} = 7$ TeV and up to 20.6 fb at $\sqrt{s} = 8$ TeV. Obtained results indicate that properties of the new particle are very similar to those predicted for the Standard Model (SM) Higgs boson [3, 4] which once again confirms the triumph of this Model. However, in spite of its beauty and capability of explaining vast amount of experimental results in particle physics SM has several drawbacks, e.g. zero neutrino masses, no dark matter candidate, hierarchy problem etc.. We are forced to believe that SM is a part of another theory which somehow cures its problems. Supersymmetry (SUSY) is among the most prominent and attractive ideas for SM extension [5, 6]. It is interesting that the discovery of the light Higgs-like resonance being interpreted as the lightest Higgs boson h of the Minimal Supersymmetric Standard Model (MSSM) with mass of order 125 GeV is consistent with TeV scale supersymmetry. It is well known that the mass of h is bounded at tree level by Z -boson mass and to reconcile it with the observed value of the resonance mass requires sufficiently large quantum corrections [7, 8] which implies (if other Higgs bosons are heavy) either heavy stop contribution or maximal mixing in stop sector. Unobservation of light squarks at the first run of LHC experiments indicates that this indeed may be the case. On the other hand it appears that the observed resonance is too heavy to be implemented “naturally” into supersymmetric extensions [9, 10, 11, 12, 13, 14, 15].

If supersymmetry is indeed inherent to our Nature it should be spontaneously broken. In a particular model this may happen in some hidden sector which does not have any renormalizable interactions with the visible one to avoid phenomenological problems with supertrace of squared mass matrix [16]. According to supersymmetric analog of the Goldstone theorem [17] there should exist a massless fermionic degree of freedom, goldstino. Being included into supergravity framework goldstino becomes longitudinal component of gravitino with mass related to the scale of supersymmetry breaking \sqrt{F} as follows $m_{3/2} = \frac{F}{\sqrt{3}M_{Pl}}$ where M_{Pl} is the Planck mass [18]. In the simplest case goldstino appears as a fermionic component of a chiral supermultiplet and interactions of this supermultiplet with other MSSM fields are suppressed by \sqrt{F} . If the SUSY breaking scale \sqrt{F} is considerably higher than the electroweak scale than the interactions of SM particles with the hidden sector are negligible. And this is the standard setup for phenomenological consideration of supersymmetric models. For instance, for gravity mediated SUSY breaking scenarios with soft parameters of

order of TeV-scale this implies $\sqrt{F} \gtrsim 10^{11}$ GeV. In the case of gauge mediation the SUSY breaking scale can be considerably lower, but still its value is limited by $\sqrt{F} \gtrsim 50$ TeV [19].

However, it is phenomenologically possible (see, e.g. Refs. [20, 21]) to have \sqrt{F} not very far from the electroweak scale, somewhere around several TeVs. The main feature of these models is the presence of a sector responsible for SUSY breaking, i.e. goldstino and probably its scalar superpartners – sgoldstinos, in low energy spectrum. In this class of models if R-parity is conserved gravitino is the lightest supersymmetric particle (LSP) with the mass at sub-eV scale. Scalar and pseudoscalar sgoldstinos acquire nonzero masses after integrating out particles from hidden sector. It is phenomenologically possible to have them around electroweak scale. If these particles are light we have an opportunity to probe the scale of supersymmetry breaking already at present-day experiments, in particular, at the LHC. Phenomenology of different aspects of low-scale supersymmetry breaking scenario have been studied long ago. Among the most interesting signatures of these models are gravitino pair production at particle collisions [22, 23, 24, 25, 26, 27, 28, 29] and decays [30, 31, 32, 33], new contributions to FCNC decays of mesons, baryons, heavy quarks and leptons with sgoldstinos in final states [34, 35, 36, 37, 38, 39]. The collider phenomenology of sgoldstinos with masses at hundred GeV scale has been studied in [40, 41, 42, 43].

Recently, an interest to this type of models has been renewed (see, e.g. [44, 45, 46, 47, 48, 49]). One of the reasons is that these theories allow to go beyond the setup of MSSM which presently becomes strongly constrained by the LHC data. In this paper we consider possible consequences of sgoldstino mixing with particles in the Higgs sector of MSSM concentrating on the most intriguing case of mixing with the lightest Higgs boson. Interactions of sgoldstino with the Higgs boson and some aspects of the mixing between them have been discussed in Refs. [45, 47, 50, 51, 52]. In particular, it has been shown that nonrenormalizable interactions with goldstino supermultiplet result in additional contribution to the Higgs potential and as a result to change of the Higgs selfcouplings. These changes can raise the value of the lightest Higgs boson mass and on this way one try to cure naturalness problem [48]. In [50] the mixing of a heavy scalar sgoldstino with the lightest Higgs boson of MSSM has been discussed to explain the excess in $h \rightarrow \gamma\gamma$ channel previously observed by ATLAS and CMS. In the present study we discuss the case when the mixing of scalar sgoldstino with the lightest Higgs boson gives an additional considerable positive contribution to the mass of the latter. This happens if sgoldstino mass is somewhat lower than the mass of h . The most interesting consequences of this mixing are modifications of the lightest Higgs boson production rates and decays as well as presence of an additional light scalar in the low energy

spectrum. As by product we find that even small mixing can considerably change sgoldstino signatures at colliders³. We perform a scan over soft MSSM parameters in the decoupling regime, discuss constraints from LHC and other experiments, find out acceptable parameter space and calculate the signal strengths for the lightest Higgs boson and scalar sgoldstino. In particular, we find that the presence of lighter scalar sgoldstino can be consistent with small 2σ excess observed at LEP [54] in $e^+e^- \rightarrow Zh$, where $h \rightarrow b\bar{b}$ with mass around 98 GeV.

The plan of the paper is the following. In Section 2 we introduce the model, describe interactions of goldstino supermultiplet with MSSM fields and in particular with the Higgs doublets. We calculate sgoldstino-Higgs mixing under assumption of CP-conservation in this sector and discuss the changes in coupling constants of new mass states. In Section 3 we describe the general strategy which we use to explore this scenario and discuss obtained results. In section 4 we present our conclusions. In Appendix A we present several auxiliary formulas.

2 The low-scale SUSY breaking model

2.1 The model description and sgoldstino-Higgs sector

In this section we describe a supersymmetric model within low-scale supersymmetry breaking framework. Let us introduce goldstino chiral superfield as $\Phi = \phi + \sqrt{2}\theta\tilde{G} + F_\phi\theta^2$, where \tilde{G} is goldstino, ϕ represents its scalar components, sgoldstinos, and F_ϕ is auxiliary field. We suppose that due to some dynamics in the hidden sector the auxiliary field F_ϕ acquires non-zero vacuum expectation value $\langle F_\phi \rangle$ and SUSY becomes spontaneously broken. Interactions of goldstino supermultiplet with MSSM are introduced in such a way that after the spontaneous supersymmetry breaking the standard set of soft terms appears (see [55, 56, 57] and references therein). Thus, we introduce the following lagrangian

$$\mathcal{L}_{\Phi-MSSM} = \mathcal{L}_{K\ddot{a}hler} + \mathcal{L}_{superpotential} . \quad (2.1)$$

Here the contribution from Kahler potential has the form

$$\mathcal{L}_{K\ddot{a}hler} = \int d^2\theta d^2\bar{\theta} \sum_k \left(1 - \frac{m_k^2}{F^2} \Phi^\dagger \Phi\right) \Phi_k^\dagger e^{g_1 V_1 + g_2 V_2 + g_3 V_3} \Phi_k , \quad (2.2)$$

³Similar well known example is the mixing of radion with the Higgs boson in models with extra dimensions [53].

where k runs over all matter and Higgs supermultiplets, and the contributions from superpotential look as

$$\begin{aligned} \mathcal{L}_{superpotential} = & \int d^2\theta \left\{ \epsilon_{ij} \left(\left(\mu - \frac{B}{F} \Phi \right) H_d^i H_u^j + \left(Y_{ab}^L + \frac{A_{ab}^L}{F} \Phi \right) L_a^j E_b^c H_d^i \right. \right. \\ & + \left. \left(Y_{ab}^D + \frac{A_{ab}^D}{F} \Phi \right) Q_a^j D_b^c H_d^i + \left(Y_{ab}^U + \frac{A_{ab}^U}{F} \Phi \right) Q_a^i U_b^c H_u^j \right) \\ & \left. + \frac{1}{4} \sum_{\alpha} \left(1 + \frac{M_{\alpha}}{F} \Phi \right) Tr W^{\alpha} W^{\alpha} \right\} + h.c., \end{aligned} \quad (2.3)$$

where α labels all the SM gauge fields, $\epsilon_{12} = -1$. The physics of goldstino supermultiplet can be described by the following effective lagrangian

$$\mathcal{L}_{\Phi} = \int d\theta^2 d\bar{\theta}^2 \left(\Phi^+ \Phi + \tilde{K}(\Phi^+, \Phi) \right) - \left(\int d\theta^2 F \Phi + h.c. \right). \quad (2.4)$$

Here we single out the standard kinetic term $\Phi^+ \Phi$ from total Kähler potential while $\tilde{K}(\Phi^+, \Phi)$ represents higher dimension contributions. The above lagrangian should be considered as an effective field theory⁴ which is valid at energies $E \lesssim \sqrt{F}$ and we consider higher order terms in $\tilde{K}(\Phi^+, \Phi)$ as suppressed by powers of F . The linear superpotential triggers spontaneous supersymmetry breaking $\langle F_{\phi} \rangle = F + \mathcal{O}(\frac{1}{F})$. In what follows we take all soft parameters, μ and F to be real and thus neglect possible CP-violation.

Let us consider the scalar sector of the model in details. By integrating out auxiliary fields of two Higgs doublets, goldstino supermultiplet and D -terms of vector superfields we obtain the tree level scalar potential for the sector of the Higgs fields and sgoldstinos in the following form

$$V = V_D + V_H + V_{\Phi}, \quad (2.5)$$

where

$$\begin{aligned} V_D = & \frac{g_1^2}{8} \left(1 + \frac{M_1}{F} (\phi + \phi^*) \right)^{-1} \left[h_d^{\dagger} h_d - h_u^{\dagger} h_u - \frac{\phi^* \phi}{F^2} (m_{h_d}^2 h_d^{\dagger} h_d - m_{h_u}^2 h_u^{\dagger} h_u) \right]^2 \\ & + \frac{g_2^2}{8} \left(1 + \frac{M_2}{F} (\phi + \phi^*) \right)^{-1} \left[h_d^{\dagger} \sigma^a h_d + h_u^{\dagger} \sigma^a h_u - \frac{\phi^* \phi}{F^2} (m_{h_d}^2 h_d^{\dagger} \sigma^a h_d - m_{h_u}^2 h_u^{\dagger} \sigma^a h_u) \right]^2, \end{aligned} \quad (2.6)$$

⁴ The lagrangian (2.1) does not contain full set of operators consistent with symmetries even to the leading order in $1/F$ because we limit ourselves only with the simplest set of terms which produce the MSSM soft parameters after SUSY breaking. Also here we face with an ambiguity: the soft term $-B\epsilon_{ij}H_d^iH_u^j$ in MSSM lagrangian can be generated not only from the superpotential as in Eq. (2.3) but also from the term $-\frac{B}{F^2}\Phi^{\dagger}\Phi\epsilon_{ij}H_d^iH_u^j|_{\theta^2\bar{\theta}^2}$ in the Kähler potential. This is related to possibility of analytic superfield redefinitions, discussed in [56].

$$V_H = \left(1 - \frac{m_{h_u}^2}{F^2} \phi^* \phi\right)^{-1} \left| \mu \epsilon_{ij} h_d^i - \frac{m_{h_u}^2}{F} \phi h_{uj}^* - \frac{B}{F} \phi \epsilon_{ij} h_d^i \right|^2 + \left(1 - \frac{m_{h_d}^2}{F^2} \phi^* \phi\right)^{-1} \left| \mu \epsilon_{ij} h_u^j - \frac{m_{h_d}^2}{F} \phi h_{di}^* - \frac{B}{F} \phi \epsilon_{ij} h_u^j \right|^2, \quad (2.7)$$

$$V_\Phi = \left(1 + \frac{\partial^2 \tilde{K}(\phi, \phi^*)}{\partial \phi \partial \phi^*} - \frac{m_{h_u}^2}{F^2} h_u^\dagger h_u - \frac{m_{h_d}^2}{F^2} h_d^\dagger h_d\right)^{-1} \left| F + \frac{B}{F} \epsilon_{ij} h_d^i h_u^j \right|^2 \quad (2.8)$$

We are going to investigate squared mass matrix of neutral scalars in electroweak symmetry breaking (ESB) minimum with leading order corrections in $1/F$. In general electroweak symmetry breaking minimum of the scalar potential allows for non-zero value of sgoldstino field ϕ because it is a singlet with respect to the SM gauge group. In what follows we consider a case study and simplify matters by assuming that $\langle \phi \rangle = 0$ in ESB minimum of the potential⁵. This can be easily obtained by tuning third derivatives of $\tilde{K}(\phi, \phi^*)$ as follows

$$\frac{\partial^3 \tilde{K}(0, 0)}{\partial \phi^* \partial \phi^2} = \quad (2.9)$$

$$\frac{1}{F^3} \left(\mu(m_{h_u}^2 + m_{h_d}^2) h_u^0 h_d^0 - \frac{M_2 g^2 + M_1 g'^2}{8} (|h_u^0|^2 - |h_d^0|^2)^2 - B \mu (|h_u^0|^2 + |h_d^0|^2) \right)$$

up to higher order corrections in $1/F$. After making this assumption we can expand scalar fields around electroweak breaking minima as follows [6]

$$h_u^0 = v_u + \frac{1}{\sqrt{2}} (h \cos \alpha + H \sin \alpha) + \frac{i}{\sqrt{2}} A \cos \beta, \quad (2.10)$$

$$h_d^0 = v_d + \frac{1}{\sqrt{2}} (-h \sin \alpha + H \cos \alpha) + \frac{i}{\sqrt{2}} A \sin \beta, \quad (2.11)$$

$$\phi = \frac{1}{\sqrt{2}} (s + ip) \quad (2.12)$$

Here $v \equiv \sqrt{v_u^2 + v_d^2} = 174$ GeV and $\tan \beta = \frac{v_u}{v_d}$ are introduced. The mixing angle α between h and H is defined by the following relations

$$\frac{\sin 2\alpha}{\sin 2\beta} = - \left(\frac{m_H^2 + m_h^2}{m_H^2 - m_h^2} \right), \quad \frac{\tan 2\alpha}{\tan 2\beta} = \left(\frac{m_A^2 + m_Z^2}{m_A^2 - m_Z^2} \right) \quad (2.13)$$

⁵ We note that nonzero v.e.v. of ϕ in particular results in deviations of the Higgs couplings to SM fermions, see e.g. [47].

with standard tree level Higgs mass parameters

$$m_A^2 = \frac{2B}{\sin 2\beta} = 2\mu^2 + m_{h_u}^2 + m_{h_d}^2, \quad (2.14)$$

$$m_{h,H}^2 = \frac{1}{2} \left(m_A^2 + m_Z^2 \mp \sqrt{(m_A^2 - m_Z^2)^2 + 4m_Z^2 m_A^2 \sin 2\beta} \right). \quad (2.15)$$

In the chosen field basis (2.10)-(2.12) the squared mass matrices can be written in the following form

$$\mathcal{M}_s^2 = \begin{pmatrix} m_H^2 & 0 & 2Y \\ 0 & m_h^2 & 2X \\ 2Y & 2X & m_s^2 \end{pmatrix} \quad (2.16)$$

for scalars and

$$\mathcal{M}_p^2 = \begin{pmatrix} m_A^2 & 2Z \\ 2Z & m_p^2 \end{pmatrix} \quad (2.17)$$

for pseudoscalars. The mixing terms $2X$, $2Y$ and $2Z$ are calculated below (2.22)- (2.24). With the assumption about zero v.e.v. of ϕ one finds that the only new contributions from SUSY breaking sector to the tree level masses of the Higgs fields come from the term V_Φ in the scalar potential. Another benefit of this assumption is that mixing terms between sgoldstino and Higgses appear from linear in ϕ part of the scalar potential. The diagonal mass squared elements for the Higgs fields read (c.f. [45])

$$m_h^2 = m_Z^2 \cos^2 2\beta + \frac{v^2}{F^2} (B \sin 2\beta - 2\mu^2)^2, \quad (2.18)$$

$$m_H^2 = m_Z^2 \sin^2 2\beta + m_A^2, \quad m_A^2 = \frac{2B}{\sin 2\beta} + 2v^2 \frac{B}{F^2} \left(B - \frac{\mu^2}{\sin 2\beta} \right). \quad (2.19)$$

As compared to the MSSM case the masses get additional contributions from new term [44, 45, 47, 51] of the fourth order in Higgs doublets

$$V_F = \frac{1}{F^2} \left| m_{h_u}^2 h_u^\dagger h_u + m_{h_d}^2 h_d^\dagger h_d - B \epsilon_{ij} h_d^i h_u^j \right|^2 \quad (2.20)$$

which comes from the part (2.8) of the scalar potential. The expressions for m_s^2 and m_p^2 can be easily obtained from Eq. (2.5) and are related to the fourth order derivatives of the Kähler potential $\tilde{K}(\phi^\dagger, \phi)$.

To obtain the off-diagonal elements in the mass matrices we expand the scalar potential to the leading order in $1/F$ and keep only the terms which are linear in sgoldstino field ϕ .

For this part of the potential we find

$$V_{mix} = \frac{\phi}{F} \left(\mu(m_u^2 + m_d^2) h_u^0 h_d^0 - \frac{g_1^2 M_1 + g_2^2 M_2}{8} (|h_u^0|^2 - |h_d^0|^2)^2 - B\mu(|h_u^0|^2 + |h_d^0|^2) \right) + h.c. \quad (2.21)$$

and for off-diagonal terms in (2.16) and (2.17) we obtain

$$X = 2\mu^3 v \sin 2\beta + \frac{1}{2} v^3 (g_1^2 M_1 + g_2^2 M_2) \cos^2 2\beta, \quad (2.22)$$

$$Y = \mu v (m_A^2 - 2\mu^2) + \frac{1}{4} (g_1^2 M_1 + g_2^2 M_2) \sin 4\beta, \quad (2.23)$$

$$Z = -\mu v (m_A^2 - 2\mu^2) \cos 2\beta. \quad (2.24)$$

In what follows we concentrate on the decoupling limit, i.e. $m_A \gg m_h$. Then all the Higgs bosons except for the lightest one become heavy. This limit corresponds to $\cos \alpha = \sin \beta$, $\sin \alpha = -\cos \beta$ in Eqs. (2.10) and (2.11). Next, we consider the scalar sgoldstino squared mass parameter m_s^2 to be somewhat less than m_h^2 . In this case the mixing between the two states can give a positive contribution to the Higgs boson mass⁶. Corresponding mass states are given by the following linear combinations

$$\tilde{h} = h \cos \theta - s \sin \theta, \quad (2.25)$$

$$\tilde{s} = h \sin \theta + s \cos \theta. \quad (2.26)$$

and the expressions for their masses squared look (in the case $m_h > m_s$) as

$$m_{\tilde{h}}^2 = \frac{1}{2} \left(m_s^2 + m_h^2 + \sqrt{(m_s^2 - m_h^2)^2 + \left(2\frac{X}{F}\right)^2} \right), \quad (2.27)$$

for new Higgs-like state \tilde{h} and

$$m_{\tilde{s}}^2 = \frac{1}{2} \left(m_s^2 + m_h^2 - \sqrt{(m_s^2 - m_h^2)^2 + \left(2\frac{X}{F}\right)^2} \right). \quad (2.28)$$

for new sgoldstino-like state \tilde{s} . The mixing angle is given by following relation

$$\tan 2\theta = \frac{2X}{F(m_s^2 - m_h^2)}. \quad (2.29)$$

⁶ The case when sgoldstino mass parameter is much larger than m_h has been studied in Refs. [45, 47, 50].

Expression for the mixing term X changes if we allow for nonzero v.e.v. of sgoldstino field.

Also note that if other Higgs bosons are also light the mixing pattern becomes more complicated. We finish this subsection by reminding that interactions of the lightest Higgs boson with (s)quarks result in the large quantum correction δ to its mass squared. This can be taken into account in the expressions above by replacement $m_h^2 \rightarrow m_h^2 + \delta$.

2.2 Sgoldstino and Higgs boson couplings

Here we write down the couplings of new mass states \tilde{h} and \tilde{s} to the SM particles. Mainly we are interested in their couplings to the SM vector bosons and heavy fermions of the third generation. Corresponding effective lagrangian for h reads

$$\begin{aligned} \mathcal{L}_h^{eff} = & \frac{2m_W^2}{\sqrt{2}v} C_W h W_\mu^+ W^{\mu-} + \frac{2m_Z^2}{\sqrt{2}v} C_Z h Z_\mu Z^\mu - \frac{m_\tau}{\sqrt{2}v} C_\tau h \bar{\tau} \tau - \frac{m_t}{\sqrt{2}v} C_t h \bar{t} t \\ & - \frac{m_b}{\sqrt{2}v} C_b h \bar{b} b + g_{h^{SM}\gamma\gamma}^{1-loop} C_{\gamma\gamma} h F^{\mu\nu} F_{\mu\nu} + g_{h^{SM}gg}^{1-loop} C_{gg} h \text{tr} G^{\mu\nu} G_{\mu\nu} \end{aligned} \quad (2.30)$$

where we introduce the scaling factors C_k for the couplings relative to their SM values. Similar interaction lagrangian for the scalar sgoldstino s can be obtained from the Eq. (2.1) as follows

$$\begin{aligned} \mathcal{L}_s^{eff} = & -\frac{M_2}{\sqrt{2}F} s W^{\mu\nu*} W_{\mu\nu} - \frac{M_{ZZ}}{2\sqrt{2}} s Z^{\mu\nu} Z_{\mu\nu} - \frac{A_{33}^L v_d}{\sqrt{2}F} s \bar{\tau} \tau - \frac{A_{33}^U v_u}{\sqrt{2}F} s \bar{t} t \\ & - \frac{A_{33}^D v_d}{\sqrt{2}F} s \bar{b} b - \frac{M_{\gamma\gamma}}{2\sqrt{2}} s F^{\mu\nu} F_{\mu\nu} - \frac{M_3}{2\sqrt{2}F} s \text{tr} G^{\mu\nu} G_{\mu\nu} \end{aligned} \quad (2.31)$$

with

$$M_{ZZ} \equiv M_1 \sin^2 \theta_W + M_2 \cos^2 \theta_W, \quad M_{\gamma\gamma} \equiv M_1 \cos^2 \theta_W + M_2 \sin^2 \theta_W. \quad (2.32)$$

We see that the interaction of the lightest Higgs boson h and the scalar sgoldstino s with quarks and leptons have similar structure, so the coupling constants for the Higgs-like mass state \tilde{h} read

$$g_{h\bar{t}t} = \frac{m_t}{v\sqrt{2}} C_t \cos \theta - \frac{A_{33}^U v \sin \beta}{\sqrt{2}F} \sin \theta, \quad (2.33)$$

$$g_{h\bar{b}b} = \frac{m_b}{v\sqrt{2}} C_b \cos \theta - \frac{A_{33}^D v \cos \beta}{\sqrt{2}F} \sin \theta, \quad (2.34)$$

$$g_{h\bar{\tau}\tau} = \frac{m_\tau}{v\sqrt{2}} C_\tau \cos \theta - \frac{A_{33}^L v \cos \beta}{\sqrt{2}F} \sin \theta. \quad (2.35)$$

The scaling factors C_t, C_b and C_τ are determined by the mixing of h and H and in the decoupling limit $m_H \gg m_h$ are close to unity, c.f. (2.10), (2.11) and (2.13).

The effective couplings of the SM Higgs boson with gluons and photons result from loop contributions of quarks and W -bosons. The scaling factors $C_{\gamma\gamma}$ and C_{gg} in (2.30) take into account additional corrections from interactions with squarks, charginos etc. which are typically suppressed if these superpartners are heavy. For scalar sgoldstino the couplings to photons and gluons appear already at tree level, see (2.31), and putting them all together one obtains for \tilde{h}

$$g_{\tilde{h}\gamma\gamma} = g_{h^{SM}\gamma\gamma}^{1-loop} C_{\gamma\gamma} \cos \theta + \frac{M_{\gamma\gamma}}{2\sqrt{2}F} \sin \theta, \quad (2.36)$$

$$g_{\tilde{h}gg} = g_{h^{SM}gg}^{1-loop} C_{gg} \cos \theta + \frac{M_3}{2\sqrt{2}F} \sin \theta, \quad (2.37)$$

where dominant SM loop contributions look as follows [3]

$$g_{h^{SM}\gamma\gamma}^{1-loop} = \frac{\alpha}{4\sqrt{2}\pi v} (\mathcal{A}_1(\tau_W) + N_c Q_t^2 \mathcal{A}_{1/2}(\tau_t)), \quad (2.38)$$

$$g_{h^{SM}gg}^{1-loop} = \frac{3}{4} \frac{\alpha_s}{6\sqrt{2}\pi v} (\mathcal{A}_{1/2}(\tau_t) + \mathcal{A}_{1/2}(\tau_b)). \quad (2.39)$$

Here $\tau_i = \frac{4m_i^2}{m_h^2}$ and loop formfactors read

$$\mathcal{A}_{1/2} = 2\tau (1 + (1 - \tau)f(\tau)), \quad (2.40)$$

$$\mathcal{A}_1 = -(2 + 3\tau + 3\tau(2 - \tau)f(\tau)), \quad (2.41)$$

with

$$f(\tau) = \begin{cases} \arcsin^2(1/\sqrt{\tau}), & \tau \geq 1, \\ -\frac{1}{4} \log \frac{1+\sqrt{1-\tau}}{1-\sqrt{1-\tau}}, & \tau < 1 \end{cases}. \quad (2.42)$$

Interactions with W and Z bosons are described by different operators for the Higgs boson and scalar sgoldstino, see Eqs (2.30) and (2.31). Corresponding couplings for new Higgs-like mass state will have the following form in the momentum space

$$g_{hZZ}^{\mu\nu} = g_{hZZ}^{\mu\nu} C_Z \cos \theta + \frac{M_{ZZ}}{2\sqrt{2}F} 2 ((k_{Z_1}, k_{Z_2})\eta^{\mu\nu} - k^{Z_2\mu} k^{Z_1\nu}) \sin \theta \quad (2.43)$$

$$g_{hW^+W^-}^{\mu\nu} = g_{hW^+W^-}^{\mu\nu} C_W \cos \theta + \frac{M_2}{2\sqrt{2}F} 2 ((k_{W^+}, k_{W^-})\eta^{\mu\nu} - k^{W^-\mu} k^{W^+\nu}) \sin \theta \quad (2.44)$$

The scaling factors C_W and C_Z are again close to unity in the decoupling regime. Effective coupling constants for sgoldstino-like state \tilde{s} can be obtained from those above by the replacement $\cos \theta \rightarrow \sin \theta$ and $\sin \theta \rightarrow -\cos \theta$.

3 Analysis of the model

3.1 Strategy for analysis

In this Section we discuss phenomenological implications of sgoldstino-Higgs mixing in context of the setup described above. For a given point in parameter space of the model which is characterized by MSSM parameters, scalar sgoldstino mass term m_s^2 and the scale of supersymmetry breaking \sqrt{F} one can ask whether this point is compatible with experimental data and in particular with results of LHC experiments. To explore this scenario we perform a scan over MSSM parameters space. In what follows we consider two parameter sets for comparison:

- *Set 1.* $1.5 < \tan \beta < 50.0$, $100 \text{ GeV} < |\mu| < 1500 \text{ GeV}$, $100 \text{ GeV} < |M_1| < 500 \text{ GeV}$, $200 \text{ GeV} < |M_2| < 500 \text{ GeV}$, $1.5 \text{ TeV} < |M_3| < 2.0 \text{ TeV}$, $|A_{33}^{U,D,E}| < 1.5 \text{ TeV}$, $700 \text{ GeV} < m_{Q_3}, m_{U_3}, m_{D_3} < 1.3 \text{ TeV}$.
- *Set 2.* This region has higher upper borders: $100 \text{ GeV} < |\mu| < 2000 \text{ GeV}$, $100 \text{ GeV} < |M_1| < 2000 \text{ GeV}$, $200 \text{ GeV} < |M_2| < 2000 \text{ GeV}$, $1.5 \text{ TeV} < |M_3| < 4.0 \text{ TeV}$, $|A_{33}^{U,D,E}| < 4 \text{ TeV}$, $700 \text{ GeV} < m_{Q_3}, m_{U_3}, m_{D_3} < 5 \text{ TeV}$.

All the MSSM parameters have been chosen at the electroweak scale. Other SUSY soft masses, which are not relevant for our analysis, are taken to be sufficiently large. In particular, given that we would like to consider decoupling regime, the Higgs pseudoscalar is also taken also to be heavy. The main difference between the two sets which will be important to us is that without additional contribution only very small fraction of models within *Set 1* provides the lightest Higgs boson with the mass higher than about 123 GeV. On the contrary *Set 2* includes rather large values of trilinear couplings A_{33}^U and stop mass parameters m_{Q_3}, m_{U_3} and larger values of m_h (up to 128 GeV) can be obtained. For supersymmetry breaking scale we fix the value $\sqrt{F} = 10 \text{ TeV}$; later on we comment about this choice. For calculation of MSSM spectra and the lightest Higgs boson coupling constants without contribution of sgoldstino sector we use package NMSSMTools [58] in the MSSM regime. We remind reader that in the scenario of low-scale supersymmetry breaking gravitino is LSP. By default NMSSMTools package in the regime of general NMSSM excludes models where neutralino is not LSP, so we turn this option off in the program. We scan over the chosen parameter spaces and exclude unphysical models by checks for absence of unphysical global minimum of the scalar potential in Higgs sector. On this stage we use a set of experimental constraints implemented in NMSSMTools, including constraints from measurements of

$\text{Br}(b \rightarrow s\gamma)$ and $\text{Br}(B_s \rightarrow \mu^+\mu^-)$ [59]. Note, that we do not impose the condition that the SUSY contribution to the anomalous magnetic moment of muon should explain the present 3σ difference between SM prediction and BNL result. The result of the scan is the spectrum of superpartners, the value m_h^2 for the squared mass of the lightest Higgs boson including MSSM quantum corrections and coupling constants of h to photons, gluons, quarks and leptons which we use in the following analysis.

Then we turn on mixing with sgoldstino as follows. We randomly scan over sgoldstino mass parameter m_s in the interval $(m_h - x, m_h)$ where $x = 35$ GeV. Such narrow interval was taken to enhance the mixing angle (2.29). We accept the model if resulting mass of the Higgs-like resonance \tilde{h} falls in the range $123 \text{ GeV} < m_{\tilde{h}} < 127 \text{ GeV}$.

Now let us discuss collider constraints which are relevant for our study. We start with the LHC data. Detailed determination of the limits on the masses of superpartners for the low-scale supersymmetry breaking scenario lies beyond the scope of this study. Still we impose a set of constraints on masses of superpartners to omit obviously excluded points in parameter space. For chosen value $\sqrt{F} = 10$ TeV all superpartners firstly decay into SM partners and next-to lightest supersymmetric particle (NLSP) which finally decays into gravitino. With gravitino LSP LHC signatures from the searches for superpartners will be the same as for general gauge mediation models [60, 61]. Below we impose a set of constraints depending on the type of NLSP which can be in our case the lightest neutralino χ_1^0 or 3rd generation squark, \tilde{t}_1 and \tilde{b}_1 . We do not take into account an exotic case of χ_1^\pm , which has been studied in [62]. Finally, only very small number of models in our scan have gluino NLSP and we neglect them completely for simplicity.

If NLSP is bino-like neutralino it decays mainly as $\tilde{\chi}_1^0 \rightarrow \gamma\tilde{G}$. Corresponding signal events have (multi)photon and missing E_T signatures [63]. This type of searches at ATLAS and CMS results in rather stringent limits on masses of superpartners: for squarks and gluinos from 1.4 to 2 TeV [64, 65, 66]. However in their analysis it has been assumed that all squarks have the same mass and they decay directly to bino-like NLSP, so for our sets of parameters the constraints should be considerably weaker and we use here conservative bound 1.4 TeV on squarks masses. Limits on masses of the lightest wino-like chargino and χ_2^0 (if they are degenerate) are about 600 – 700 GeV [64] independently of χ_1^0 mass and we used in this case the strongest constraint. For the case of wino-like or higgsino NLSP neutralino it decays mainly into Z and/or h . Searches for a diphoton, $Z + \gamma$, $W + \gamma$ and/or jets and E_T^{miss} signatures [65] result in the limits 900 – 2000 GeV for gluino and squark masses. Again here only a simplified case of degenerate squarks has been considered. The

limit on mass of NLSP neutralino χ_1^0 in this case depends on branchings of χ_1^0 decay into $Z\tilde{G}$ and $h\tilde{G}$ and varies [67, 68] from 380 GeV for $\text{Br}(\chi \rightarrow Z\tilde{G}) = 1$ to zero for $\text{Br}(\chi \rightarrow h\tilde{G}) = 1$. Here we impose the strongest constraint by assuming that NLSP decays to Z boson pair with 100% branching ratio. When a squark is NNLSP and wino-like neutralino is NLSP we take into account constraints from cascade production of NLSP- lightest neutralino via stop $m_{\tilde{t}_1} > 560$ GeV [69] and sbottom $m_{\tilde{b}_1} > 470$ GeV [70] squarks. In the case of squark (\tilde{t}_1 or \tilde{b}_1) NLSP we impose the following bounds from searches for direct pair production of sbottom $m_{\tilde{t}_1} > 650$ GeV [71] and stop $m_{\tilde{t}_1} > 760$ GeV [72] squarks. Somewhat arbitrarily we impose a stringent bound on gluino mass $M_3 > 1.5$ TeV for all the cases. We comment about influence of this constraint below.

For each chosen model we calculate predicted signal strengths $R = \sigma/\sigma_{SM}(m_{h^{SM}} = m_{\tilde{h},\tilde{s}})$, i.e. the ratio of a signal cross section for new Higgs or sgoldstino resonances to the cross section of the same process in the SM with the Higgs boson of the same mass. In the narrow width approximation for a final state f the signal strength can be written as

$$R_f = \frac{\sigma(pp \rightarrow \tilde{h}(\tilde{s}))\text{Br}(\tilde{h}(\tilde{s}) \rightarrow f)}{\sigma(pp \rightarrow h^{SM})\text{Br}(h^{SM} \rightarrow f)}, \quad (3.1)$$

where $\sigma(pp \rightarrow \tilde{h}(\tilde{s}))$ is the total production rate of the Higgs-like (sgoldstino-like) state given by sum over different production mechanisms, $\text{Br}(\tilde{h}(\tilde{s}) \rightarrow f)$ is the branching ratio of the decay of $\tilde{h}(\tilde{s})$ into final state f , while $\sigma(pp \rightarrow h^{SM})$ and $\text{Br}(h^{SM} \rightarrow f)$ are similar quantities for the SM Higgs boson with the same mass. In what follows we consider the following final states $\gamma\gamma$, ZZ , WW , $b\bar{b}$ and $\tau^+\tau^-$ which are most relevant for current LHC searches. Further, we distinguish between several dominant production mechanisms, namely gluon-gluon fusion (ggF) and vector boson fusion along with associated production with W and Z (VBF and VH) as they provide with different signatures. The signal strength (3.1) can be approximated by

$$R_f^{ggF} = \frac{\Gamma(\tilde{h} \rightarrow gg)\text{Br}(\tilde{h} \rightarrow f)}{\Gamma(h^{SM} \rightarrow gg)\text{Br}(h^{SM} \rightarrow f)} \quad (3.2)$$

for the case of ggF and as

$$R_f^{VBF/VH} = \frac{\Gamma(\tilde{h} \rightarrow WW, ZZ)\text{Br}(\tilde{h} \rightarrow f)}{\Gamma(h^{SM} \rightarrow WW, ZZ)\text{Br}(h^{SM} \rightarrow f)} \quad (3.3)$$

for VBF or VH production mechanisms. Similar expressions are used for the case of sgoldstino-like state \tilde{s} . Here we should note that interactions of sgoldstino with massive

vector bosons are governed by operator which has different structure than that for the Higgs boson. But considering kinematics of the processes of Higgs production via VBF or VH-strahlung mechanisms it is easy to convince yourself that the momentum-dependent parts of (2.44) and (2.43) give negligible contribution for parameters in the *Sets 1* and *2* in comparison with the SM parts of the couplings unless $\cos\theta$ is not too small. The widths of the decays entering (3.2) and (3.3) are calculated using formulas in Ref. [3] and replacing corresponding coupling constants with those presented above. The only exception is decays into pair of massive vector bosons. In this case for the calculation of partial widths we use results of Ref. [73] and present corresponding formulas in Appendix A for completeness. Experimental constraints on signal strengths from ATLAS and CMS results will be discussed in the next Section.

As it has been already noted gluon-gluon fusion is the most important production mechanism for $\gamma\gamma$, ZZ and WW channels. At the same time as we observed above the coupling of the Higgs boson \tilde{h} to the gluons receives tree level contribution (2.37) due to the mixing with sgoldstino. Let us require that this contribution should not dominate over the SM part. It can be suppressed either by small mixing angle or by sufficiently large \sqrt{F} . Considering the case of non-negligible mixing the sgoldstino coupling is smaller than 1-loop SM contribution when $\sqrt{F} \gtrsim \left(\frac{3\pi M_3 v}{\alpha_s}\right)^{1/2}$. Given chosen limit $M_3 \gtrsim 1.5$ TeV from the direct searches for gluinos at the LHC one finds $\sqrt{F} \gtrsim 7$ TeV. This explains our choice of sufficiently large value of supersymmetry breaking scale $\sqrt{F} = 10$ TeV. We note in passing that the real constraint on M_3 in a given model can be considerably lower with current ATLAS and CMS data. Thus, smaller values of \sqrt{F} are possible along with large sgoldstino-Higgs mixing.

Now let us turn to the discussion of sgoldstino-like state which is somewhat lighter than the Higgs-like resonance. Here we impose additional constraints from LEP [74] and Tevatron [75]. Particularly strong limits come from LEP results on Higgs boson searches [54, 74, 76] in $e^+e^- \rightarrow Zh$ with $h \rightarrow b\bar{b}$, $\tau^+\tau^-$ and $\gamma\gamma$. We remind reader that a small, about 2σ , excess has been observed at LEP in this channel around invariant mass 98 GeV of $b\bar{b}$ pair. In what follows we would like to explore interesting possibility that this sgoldstino-like state with mass around 98 GeV could be source of this excess. For such models we additionally require that the mass of \tilde{s} should be in the range 95 – 101 GeV and additionally $0.1 < R_{b\bar{b}}^{VBF/VH}(\tilde{s}) < 0.25$, see Ref. [54]. Alternative explanations of this excess have been proposed within Non-minimal Supersymmetric Standard Model (NMSSM) in papers [77, 78].

3.2 Results and discussions

Here we present results of the scan over MSSM parameter space with two sets of parameters introduced in Section 3.1. In the figures below we show the different physical quantities for phenomenologically acceptable models. Red points mark models which do not satisfy chosen

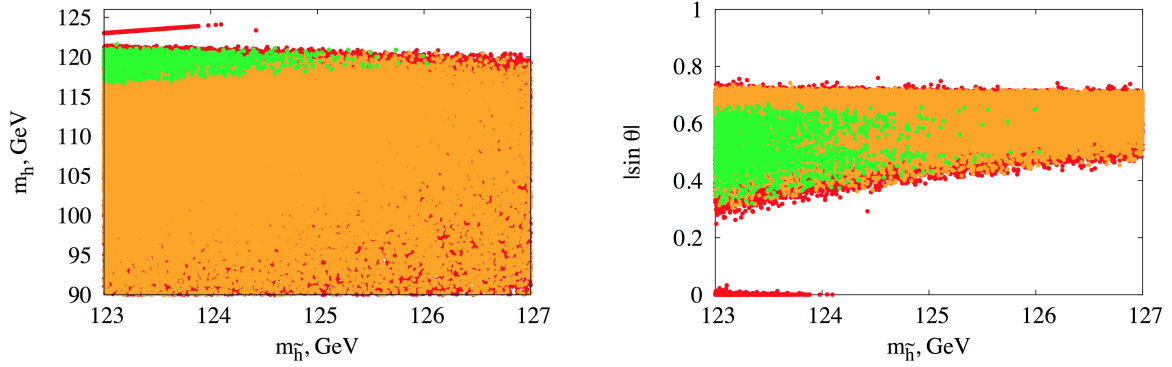


Figure 1: Scatter plots in $m_{\tilde{h}} - m_h$ (left panel) and $m_{\tilde{h}} - |\sin \theta|$ (right panel) planes for *Set 1*. Models excluded by ATLAS and CMS searches for superpartners are tagged by red color. Orange points correspond to models that satisfy LHC constraints but do not satisfy constraints from LEP experiment. Other models are shown in green.

bounds on masses of superpartners. By orange points we show models which are excluded by LEP constraints on sgoldstino-like state production in $e^+e^- \rightarrow Z\tilde{s}$ discussed above. Models which pass all these constraints are shown in green.

We start with *Set 1* of parameters. In Fig. 1 (left panel) we show distributions of models over the mass of the Higgs resonance before and after mixing. We see that without the mixing mass m_h is always below 123 GeV except for very limited number of models. The mixing with sgoldstino can increase the mass of Higgs-like state \tilde{h} till observed value. However, the number of acceptable models considerably decreases with increase of $m_{\tilde{h}}$. In Fig. 1 (right panel) we show mixing angle versus mass $m_{\tilde{h}}$. We see that for the parameter space given by *Set 1*, the Higgs-like resonance should have considerable admixture of sgoldstino with $|\sin \theta| \sim 0.4 - 0.6$ to get observable value for its mass. Thus, in the most of the acceptable models the Higgs mass reaches its observed value without large masses of stops and mixing in their sector. The models with negligible mixing with sgoldstino on the right plot correspond to those models on the left plot in which mass m_h exceeds 123 GeV. These models appear to be closed by searches for superpartners. In Fig. 2 we show the masses

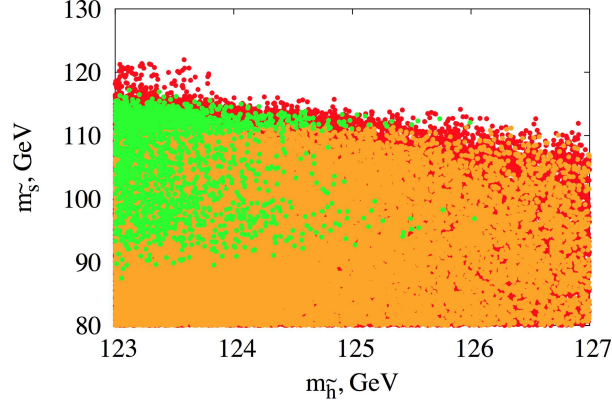


Figure 2: Scatter plot in $m_{\tilde{h}} - m_{\tilde{s}}$ plane of Set 1 data. Color notations are the same as in Fig. 1.

of Higgs-like and sgoldstino-like resonances and see that in the described setup sgoldstino with masses larger than 85 GeV is favorable. In Fig. 3 we show distributions of models on different combinations of several MSSM parameters and masses of superpartners for *Set 1* of parameters. One can see from the distribution in the parameters $\mu - \tan \beta$ (upper left panel) that large values of μ and moderate $\tan \beta$ are preferable. This can be explained from the expression for mixing in Eq. (2.22) and the Higgs boson mass (2.18) and (2.27): small μ and large $\tan \beta$ result in suppression in mixing parameter X . Smaller values of $\tan \beta$ are not favorable because tree level value of the Higgs boson mass becomes additionally suppressed, see Eq. (2.18). In the upper right plot in this Figure we show values of A_{33}^U versus μ and see that phenomenologically acceptable models have A_{33}^U near its largest value for *Set 1*. The reason is that such values of A_{33}^U increase $X_t = A_{33}^U - \mu \cot \beta$ and as a result increase 1-loop correction to Higgs mass [8]

$$\delta = \frac{3}{(4\pi)^2} \frac{m_t^4}{v^2} \left[\ln \frac{m_{\tilde{t}_1} m_{\tilde{t}_2}}{m_t^2} + \frac{X_t^2}{m_{\tilde{t}_1} m_{\tilde{t}_2}} \left(1 - \frac{X_t^2}{12 m_{\tilde{t}_1} m_{\tilde{t}_2}} \right) \right] \quad (3.4)$$

The masses of the lightest neutralino and chargino are shown in the lower left panel in Fig. 3. In the lower right panel we show the masses of lightest stop and sbottom squarks. We see that there are plenty of models in which these masses can be as light as 500 – 700 GeV what can be explored in the future LHC runs. Scatter plots similar to those in Figs. 1–3 can be obtained for the *Set 2* of parameters which is considerably wider. But in this case they are not so informative as corresponding models admit arbitrary mixing between the lightest

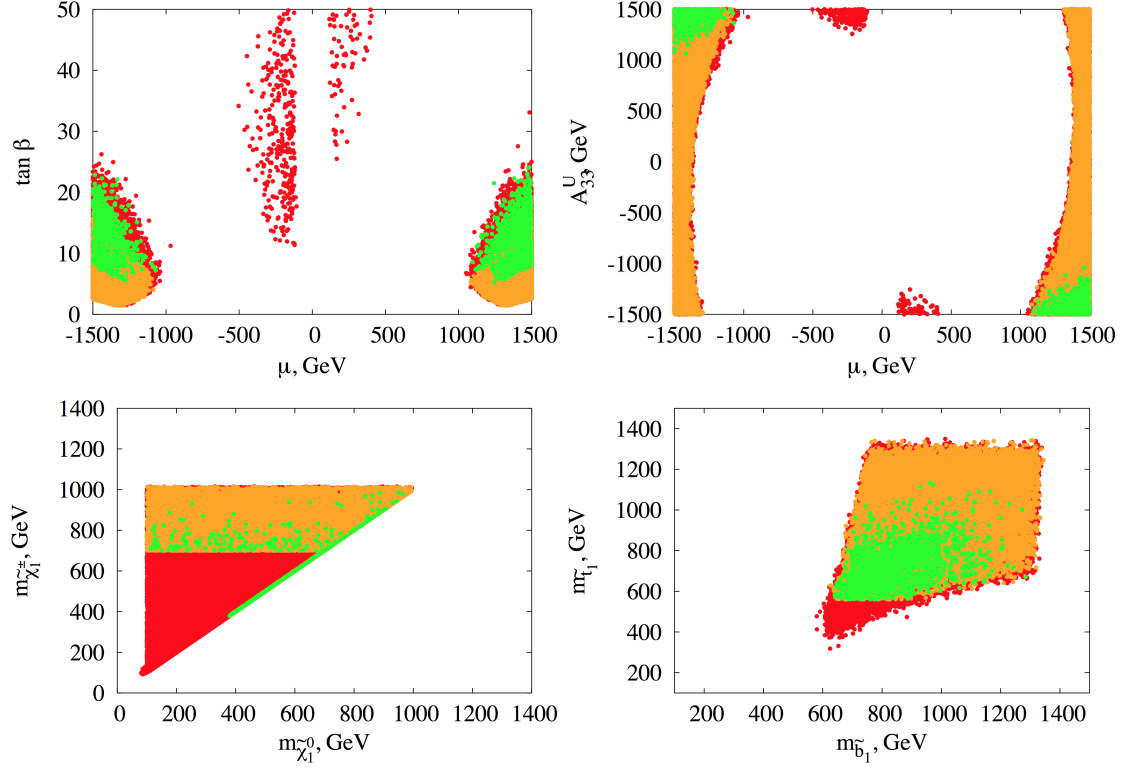


Figure 3: Scatter plots in $\mu - \tan \beta$ (upper left panel), $\mu - A_{33}^U$ (upper right panel), $m_{\tilde{\chi}_1^0} - m_{\tilde{\chi}_1^\pm}$ (lower left panel) and $m_{\tilde{b}_1} - m_{\tilde{\tau}_1}$ (lower right panel) planes for *Set 1*. Color notations are the same as in Fig. 1.

Higgs boson and scalar sgoldstino.

Now we turn to the discussion of LHC signal strengths for the Higgs-like resonance \tilde{h} . On the plots below we drop all the models excluded by the LEP constraints or LHC bounds on masses of superpartners and for remaining models we introduce constraints for signal strengths obtained by ATLAS and CMS experiments in their searches for the Higgs boson [81, 82]. Although for $\gamma\gamma$ and ZZ (WW) channels the dominating production mechanism is ggF while for $\tau\tau$ and $b\bar{b}$ channels this is VBF/VH still we conservatively impose the following constraints (obtained by unification of ATLAS and CMS results) independently of the Higgs production mechanism

$$\begin{aligned}
0.51 < R_{\gamma\gamma}^{ggF, VBF/VH}(\tilde{h}) < 1.9, \quad 0.66 < R_{ZZ}^{ggF, VBF/VH}(\tilde{h}) < 1.84, \\
0.53 < R_{WW}^{ggF, VBF/VH}(\tilde{h}) < 1.32, \quad 0.51 < R_{\tau\tau}^{ggF, VBF/VH}(\tilde{h}) < 1.9, \\
0 < R_{b\bar{b}}^{ggF, VBF/VH}(\tilde{h}) < 1.5.
\end{aligned} \tag{3.5}$$

In the figures below we show in magenta the models which satisfy the bounds (3.5). Also we mark in blue color the models in which additionally sgoldstino-like resonance can explain 98 GeV LEP excess.

We show signal strengths for the Higgs-like resonance in gluon-gluon fusion production

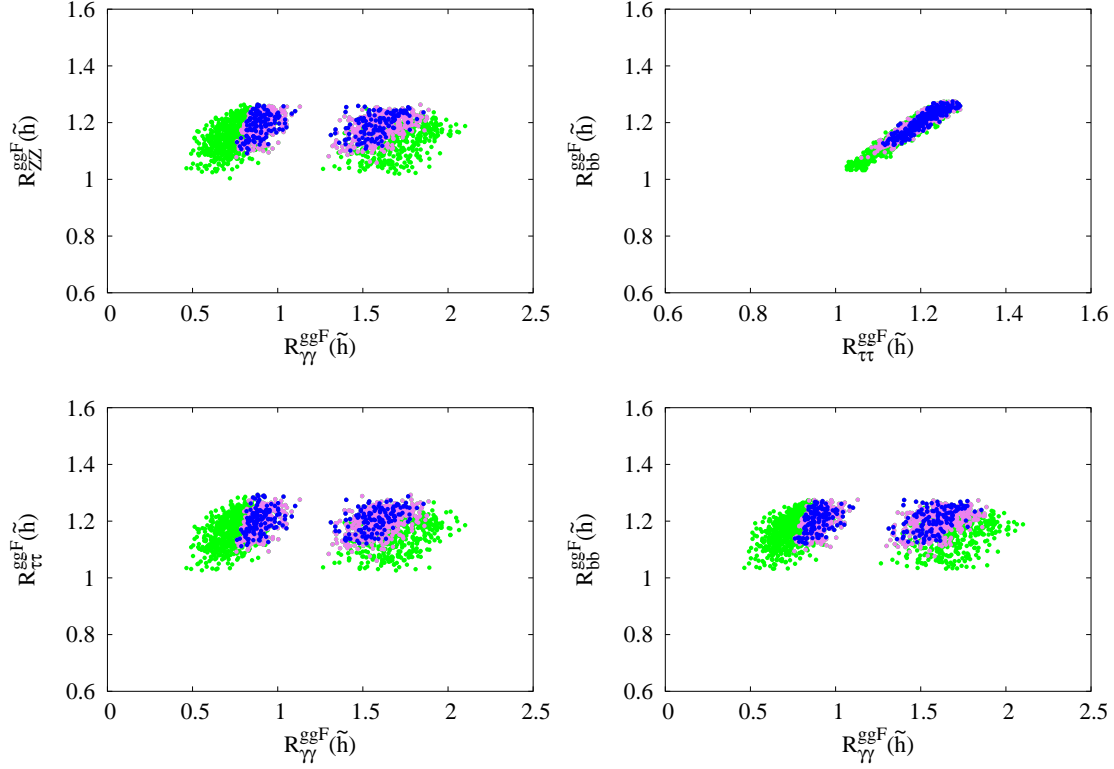


Figure 4: Scatter plots in $R_{\gamma\gamma}^{ggF}(\tilde{h}) - R_{ZZ}^{ggF}(\tilde{h})$ (upper left panel), $R_{\tau\tau}^{ggF}(\tilde{h}) - R_{bb}^{ggF}(\tilde{h})$ (upper right panel), $R_{\gamma\gamma}^{ggF}(\tilde{h}) - R_{\tau\tau}^{ggF}(\tilde{h})$ (lower left panel) and $R_{\gamma\gamma}^{ggF}(\tilde{h}) - R_{bb}^{ggF}(\tilde{h})$ (lower right panel) planes for *Set 1*. All the models satisfy both LEP constraints and LHC bounds on masses of superpartners. Models which satisfy constraints Higgs signal strength (3.5) are marked by magenta. If in addition the model contains sgoldstino-like resonance capable of explaining 98 GeV LEP excess it is shown in blue.

channel in different combinations in Fig. 4 for the *Set 1* and in Fig. 5 for *Set 2*. From the plots in Figs. 4 and 5 we see that all the signal strengths except for $R_{\gamma\gamma}^{ggF}$ are somewhat larger than unity for phenomenologically acceptable models, while for $\gamma\gamma$ channel there are two regions with higher and lower values of the signal strengths. Since sgoldstino s has tree level couplings to photons and gluons while for the Higgs boson h these couplings appear only at loop level, in general one expects large sensitivity of the couplings of Higgs-like state \tilde{h} to sgoldstino

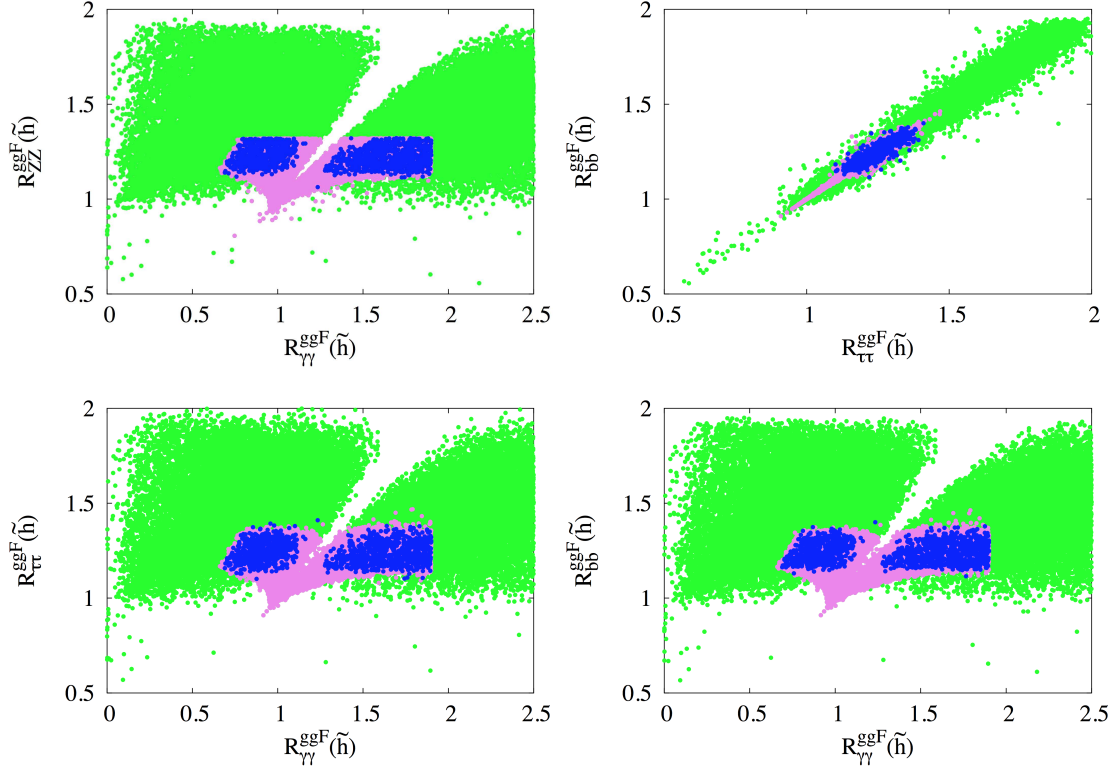


Figure 5: Scatter plots in $R_{\gamma\gamma}^{ggF}(\tilde{h}) - R_{ZZ}^{ggF}(\tilde{h})$ (upper left panel), $R_{\tau\tau}^{ggF}(\tilde{h}) - R_{bb}^{ggF}(\tilde{h})$ (upper right panel), $R_{\gamma\gamma}^{ggF}(\tilde{h}) - R_{\tau\tau}^{ggF}(\tilde{h})$ (lower left panel), $R_{\gamma\gamma}^{ggF}(\tilde{h}) - R_{bb}^{ggF}(\tilde{h})$ (lower right panel) planes for *Set 2*. The color notations are the same as in Fig. 4.

admixture and to corresponding parameters which govern these couplings, namely M_3 and $M_{\gamma\gamma}$. Depending on relative signs between the mixing angle (which is determined by the sign of μ) and soft gaugino mass parameters $M_{1,2,3}$ the couplings to gluons and photons can either increase or decrease with respect to their values without the mixing. We have found that M_3 and μ should have opposite signs for the coupling $g_{\tilde{h}gg}$ be close to experimentally observed value. With another choice of the signs the coupling of \tilde{h} to gluons becomes unacceptably small; we do not show corresponding models in all the Figures below. The signs of M_1 and M_2 can be arbitrary (we choose them of the same sign) and they correspond to two different domains for $R_{\gamma\gamma}^{ggF}$ in Figs. 4 and 5. The increase in the signal strengths for fermionic and massive vector boson channels is related to the fact that with our choice of parameters and of the signs of μ and M_3 the coupling of \tilde{h} to gluons appears to be somewhat larger than its value in SM. Hence, the production cross section in ggF increases.

Similar plots for the case of VBF and VH production mechanisms are presented in

Fig. 6 for *Set 1* and in Fig. 7 for *Set 2*. In this case the production cross section is typically

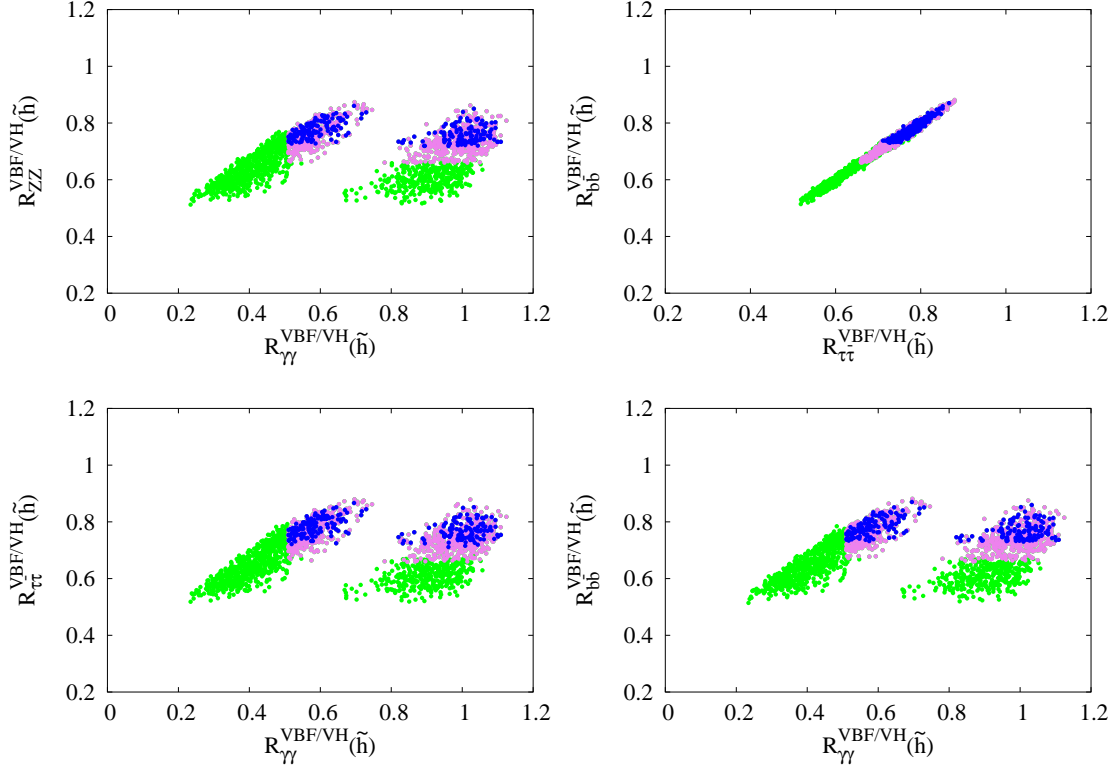


Figure 6: Scatter plots in $R_{\gamma\gamma}^{VBF/VH}(\tilde{h}) - R_{ZZ}^{VBF/VH}(\tilde{h})$ (upper left panel), $R_{\tau\tau}^{VBF/VH}(\tilde{h}) - R_{bb}^{VBF/VH}(\tilde{h})$ (upper right panel), $R_{\gamma\gamma}^{VBF/VH}(\tilde{h}) - R_{\tau\tau}^{VBF/VH}(\tilde{h})$ (lower left panel), $R_{\gamma\gamma}^{VBF/VH}(\tilde{h}) - R_{bb}^{VBF/VH}(\tilde{h})$ (lower right panel) planes of *Set 1*. The color notations are the same as in Fig. 4.

suppressed by the mixing as compared to the case of the SM Higgs boson because the contribution to the coupling with massive vector bosons from sgoldstino is small as we discuss in Section 3.1. Almost the same can be said about the couplings to heavy fermions: tree level Higgs part of the couplings in Eqs. (2.33)–(2.35) are typically larger than sgoldstino contribution for the chosen values of parameters, in particular for $\sqrt{F} = 10$ TeV. Note that due to this reason we expect that the total width of the Higgs-like resonance is suppressed by factor $\cos^2 \theta$ with respect the SM Higgs boson decay width. Summarizing, in Fig. 6 and Fig. 7 the Higgs signal strengths for fermion and massive vector boson channels in VBF/VH for most of the models become suppressed due to the mixing with sgoldstino, in particular, for models in which sgoldstino explains 98 GeV LEP excess. Also we show correlations between different production mechanisms, ggF and VBF/VH , for $\gamma\gamma$ and ZZ channels in

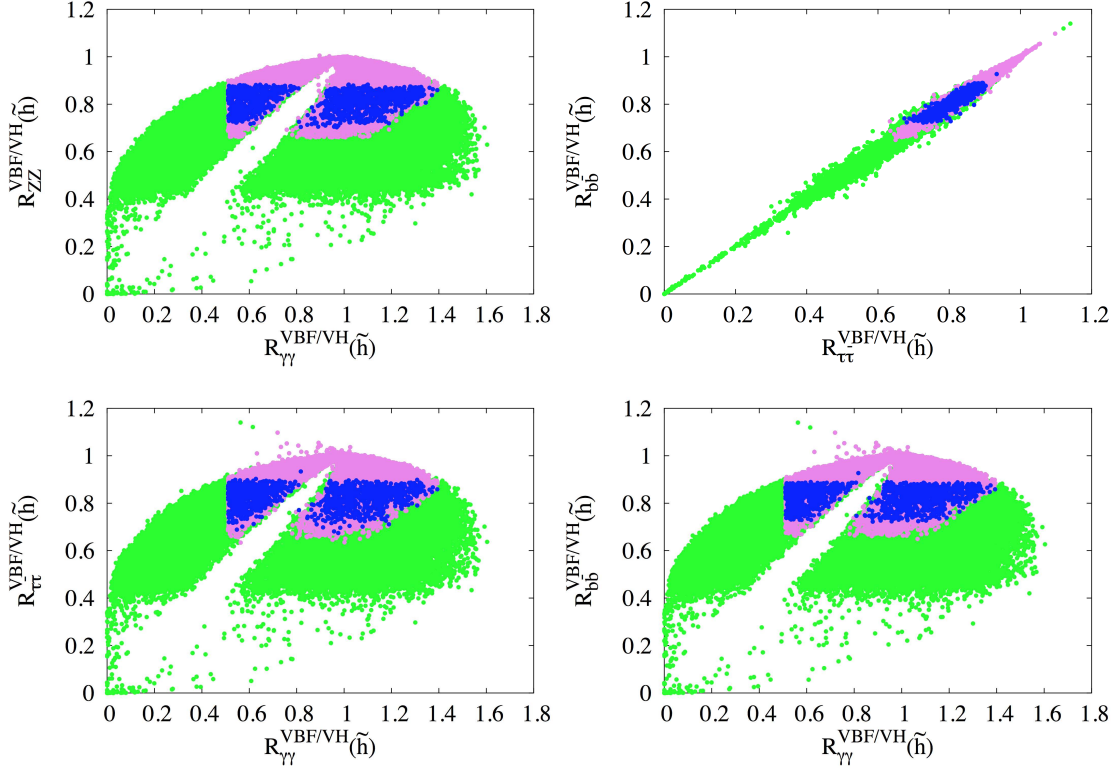


Figure 7: Scatter plots in $R_{\gamma\gamma}^{VBF/VH}(\tilde{h}) - R_{ZZ}^{VBF/VH}(\tilde{h})$ (upper left panel), $R_{\tau\tau}^{VBF/VH}(\tilde{h}) - R_{bb}^{VBF/VH}(\tilde{h})$ (upper right panel), $R_{\gamma\gamma}^{VBF/VH}(\tilde{h}) - R_{\tau\tau}^{VBF/VH}(\tilde{h})$ (lower left panel), $R_{\gamma\gamma}^{VBF/VH}(\tilde{h}) - R_{bb}^{VBF/VH}(\tilde{h})$ (lower right panel) planes for *Set 2*. The color notations are the same as in Fig. 4.

Fig. 8 for *Set 1* and in Fig. 9 for *Set 2*. Again for $\gamma\gamma$ we see two domains corresponding to different signs of $M_{1,2}$.

The general conclusion from the above discussions is that mixing of the lightest Higgs boson with a lighter sgoldstino results in an increase of signal strengths of fermionic and massive vector boson channels in ggF and in a decrease of their values in VBF/VH production mode and an increase in ZZ channel. We do not show here the signal strength for WW channel because it is almost the same as for ZZ . Additionally, requirement that the scalar sgoldstino explains LEP excess results in prediction of particular regions of R where their values deviate from unity. So an increase of accuracy of measurements of the signal strength for observed Higgs-like resonance which is expected with next LHC runs will give an opportunity to check this scenario.

Now we turn to the discussion of sgoldstino collider phenomenology with presented setup.

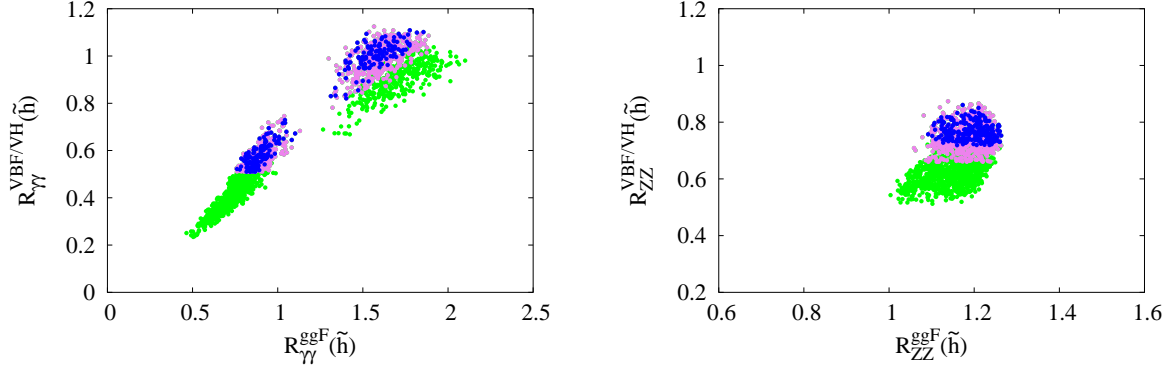


Figure 8: Scatter plots in $R_{\gamma\gamma}^{ggF}(\tilde{h}) - R_{\gamma\gamma}^{VBF/VH}(\tilde{h})$ (left panel) and $R_{ZZ}^{ggF}(\tilde{h}) - R_{ZZ}^{VBF/VH}(\tilde{h})$ (right panel) planes for *Set 1*. The color notations are the same as in Fig. 4.

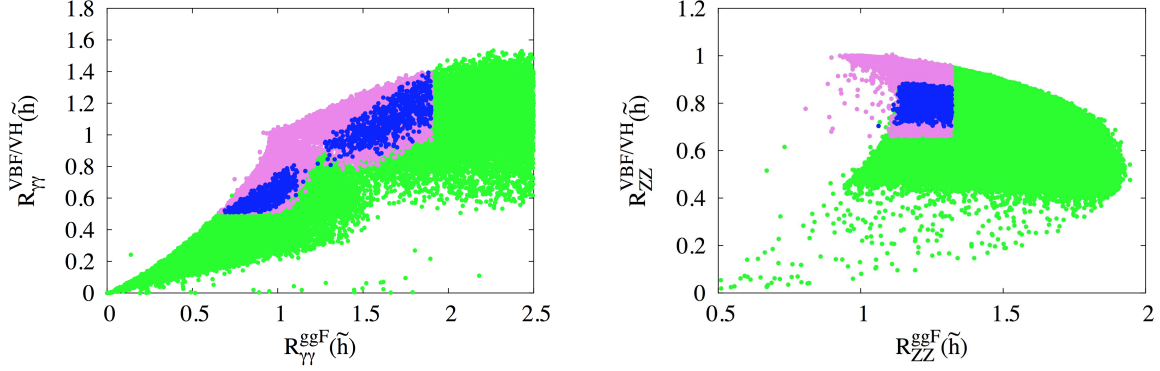


Figure 9: Scatter plots in $R_{\gamma\gamma}^{ggF}(\tilde{h}) - R_{\gamma\gamma}^{VBF/VH}(\tilde{h})$ (left panel), $R_{ZZ}^{ggF}(\tilde{h}) - R_{ZZ}^{VBF/VH}(\tilde{h})$ (right panel) planes for *Set 2*. The color notations are the same as in Fig. 4.

It has been previously studied in Refs. [31, 40, 41, 42, 43] but without including effects of its possible mixing with the Higgs boson. As we find this mixing can be extremely important. Firstly, let us discuss the main decay channels and the hierarchy between their branchings for sgoldstinos with masses at electroweak scale. In general the interactions of scalar sgoldstino with SM particles are similar to those of the lightest Higgs boson but the hierarchy between the coupling constants is quite different. The main distinction is the fact that sgoldstino couplings to gluons and photons appear already at tree level as it have been discussed in Section 2.2. That's why, for typical values of soft MSSM parameters pure sgoldstino with mass around hundred GeV dominantly decays into pair of gluons and

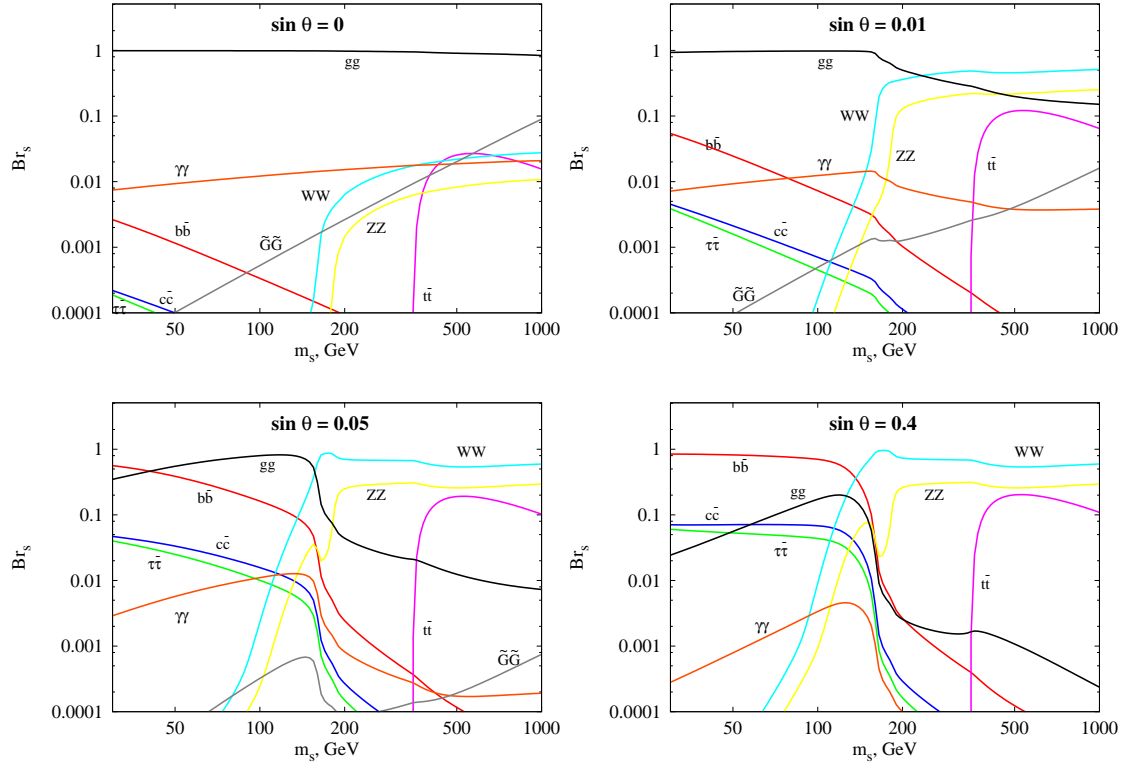


Figure 10: Modification of scalar sgoldstino branching ratios at different values of mixing angle: $\sin \theta = 0.0, 0.01, 0.05$ and 0.4 . We take the following values for MSSM soft parameters: $\sqrt{F} = 10$ TeV, $M_1 = 400$ GeV, $M_2 = 800$ GeV, $M_3 = -1200$ GeV, $A^{U,D,E} = 700$ GeV and $A_{ab}^{U,D,E} = Y_{ab}^{U,D,E} A^{U,D,E}$ where $Y_{ab}^{U,D,E}$ are MSSM Yukawa couplings.

photons which is governed by parameters M_3 and $M_{\gamma\gamma}$, respectively. Then it can decay into pairs of quarks and leptons and corresponding decay rates are governed by corresponding trilinear soft terms which enter interactions for superpartners of these quarks and leptons in (2.31). Also sgoldstinos can decay into pair of gauge bosons and these decay widths are governed by corresponding soft gaugino masses. And finally sgoldstinos can decay into pair of gravitinos, which looks as invisible decay. The hierarchy of the branching ratios depends on hierarchy of the soft terms in MSSM lagrangian. In Fig. 10 we show how the hierarchy of branching ratios for scalar sgoldstino decays changes depending on mixing angle. Again we set $\sqrt{F} = 10$ TeV and for the time being we consider here very wide interval of sgoldstino masses. We see that even small value of mixing angle drastically changes the hierarchy between possible decay channels and already at mixing angle of 0.4 the hierarchy becomes

very similar to the case of the Higgs, except for the partial widths are now suppressed by square of sine of mixing angle. This fact can considerably change the strategy of sgoldstino searches at colliders [31, 40, 41, 42, 79].

Now we return to the light sgoldstino-like state in our scenario and we show the signal strengths of \tilde{s} for $b\tilde{b}, \tau\tilde{\tau}, \gamma\gamma$ and ZZ channels in gluon-gluon fusion production process in Fig. 11 for *Set 1* and in Fig. 12 for *Set 2*. We see that for ggF production the sgoldstino

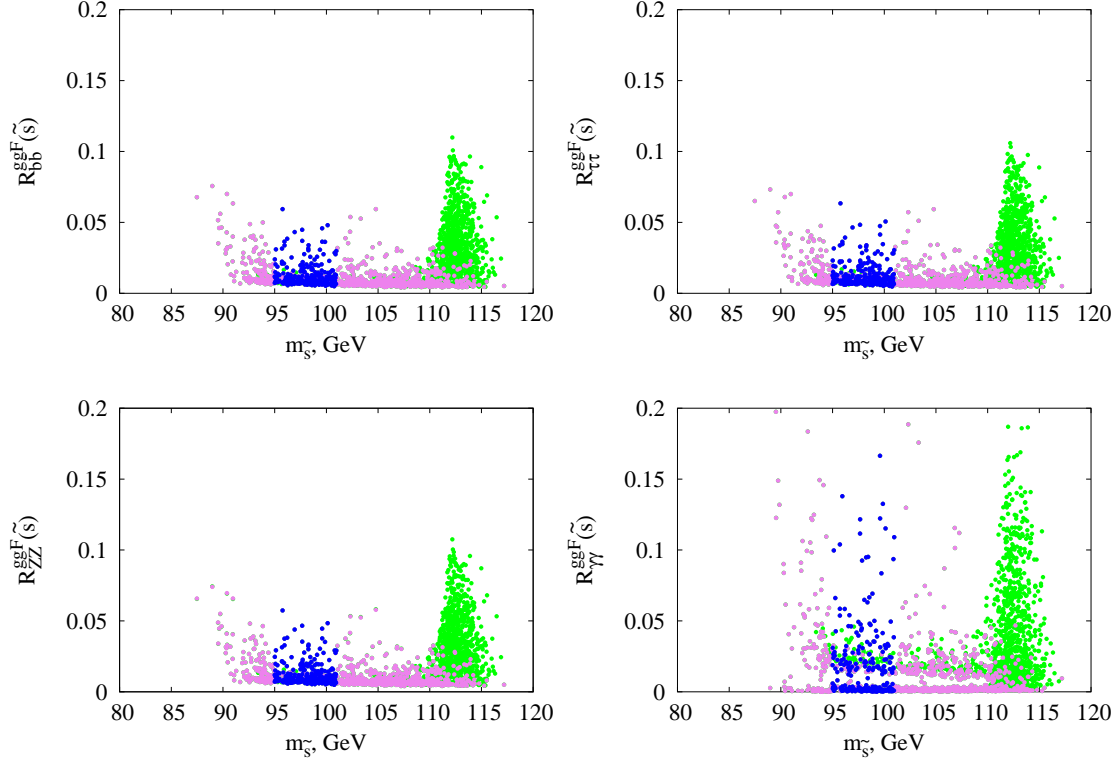


Figure 11: Scatter plots in $m_{\tilde{s}} - R_{b\tilde{b}}^{ggF}(\tilde{s})$ (upper left panel), $m_{\tilde{s}} - R_{\tau\tilde{\tau}}^{ggF}(\tilde{s})$ (upper right panel), $m_{\tilde{s}} - R_{ZZ}^{ggF}(\tilde{s})$ (lower left panel), $m_{\tilde{s}} - R_{\gamma\gamma}^{ggF}(\tilde{s})$ (lower right panel) planes for *Set 1*. The color notations are the same as in Fig. 4.

signal strength does not exceed 0.1 for fermionic and ZZ (WW) channels for *Set 1* and is less than $0.4 - 0.5$ for *Set 2*. While in the $\gamma\gamma$ channel $R_{\gamma\gamma}^{ggF}(\tilde{s})$ can reach values about 0.2 for *Set 1* and can be quite large for some models in *Set 2*. In the last case we can use results of the CMS [82] and ATLAS [83] searches for Higgs boson in $\gamma\gamma$ channel and put additional constraints on $R_f^{ggF}(\tilde{s})$. They are shown in lower right panel in Fig. 12 where all the models above red and orange curves are excluded. Other searches for the Higgs boson made by LHC and TeVatron [75] experiments put limits which do not introduce additional constraints.

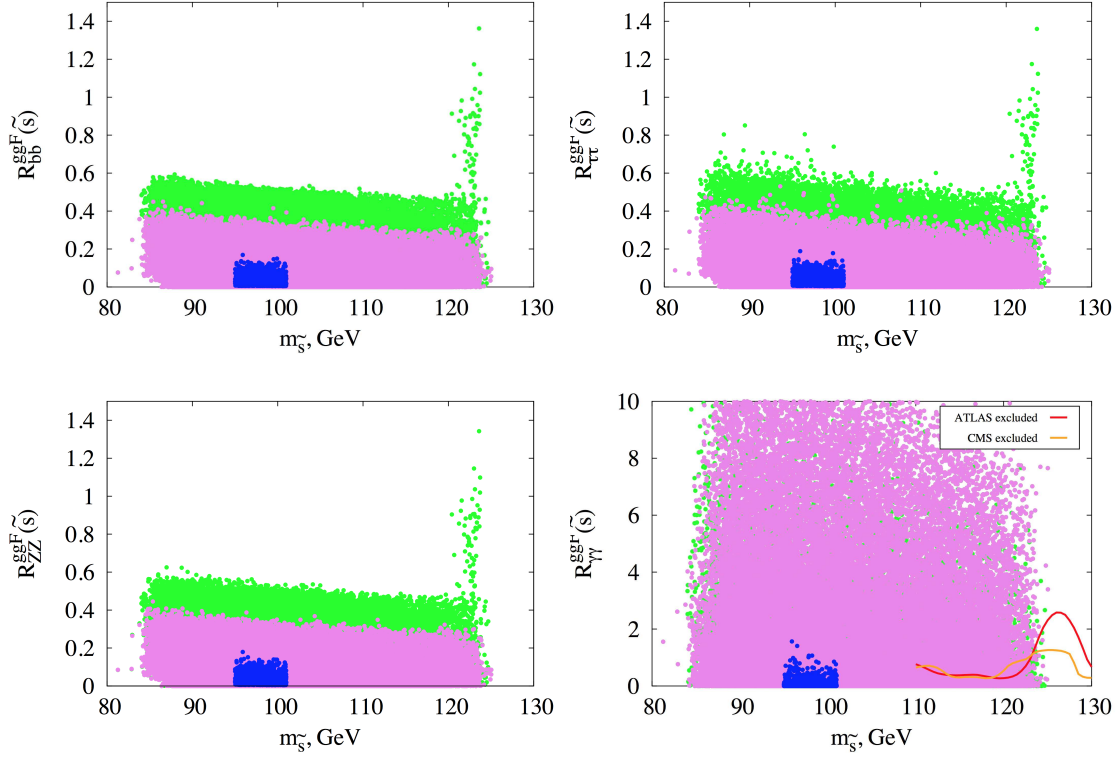


Figure 12: Scatter plots in $m_{\tilde{s}} - R_{bb}^{ggF}(\tilde{s})$ (upper left panel), $m_{\tilde{s}} - R_{\tau\tau}^{ggF}(\tilde{s})$ (upper right panel), $m_{\tilde{s}} - R_{ZZ}^{ggF}(\tilde{s})$ (lower left panel), $m_{\tilde{s}} - R_{\gamma\gamma}^{ggF}(\tilde{s})$ (lower right panel) planes for *Set 2*. The color notations are the same as in Fig. 4.

Similar scatter plots for *VBF/VH* production process are shown in Fig. 13 for the case of *Set 1* and in Fig. 14 for the case of *Set 2*. We see that the signatures of *VBF/VH* sgoldstino production look quite promising: corresponding signal strengths can reach values up to 1.2 – 1.3 for $\gamma\gamma$ and for other channels they can be as large as 0.3. This indicates that the discussed scenario is out of reach of TeVatron experiments but hopefully can be probed in the future LHC runs.

4 Concluding remarks

To summarize, in this paper we discussed implications of the possible mixing between the supersymmetric Higgs sector and hidden sector in models with low-scale supersymmetry breaking. We have found that the mixing of scalar sgoldstino \tilde{s} to the lightest Higgs boson

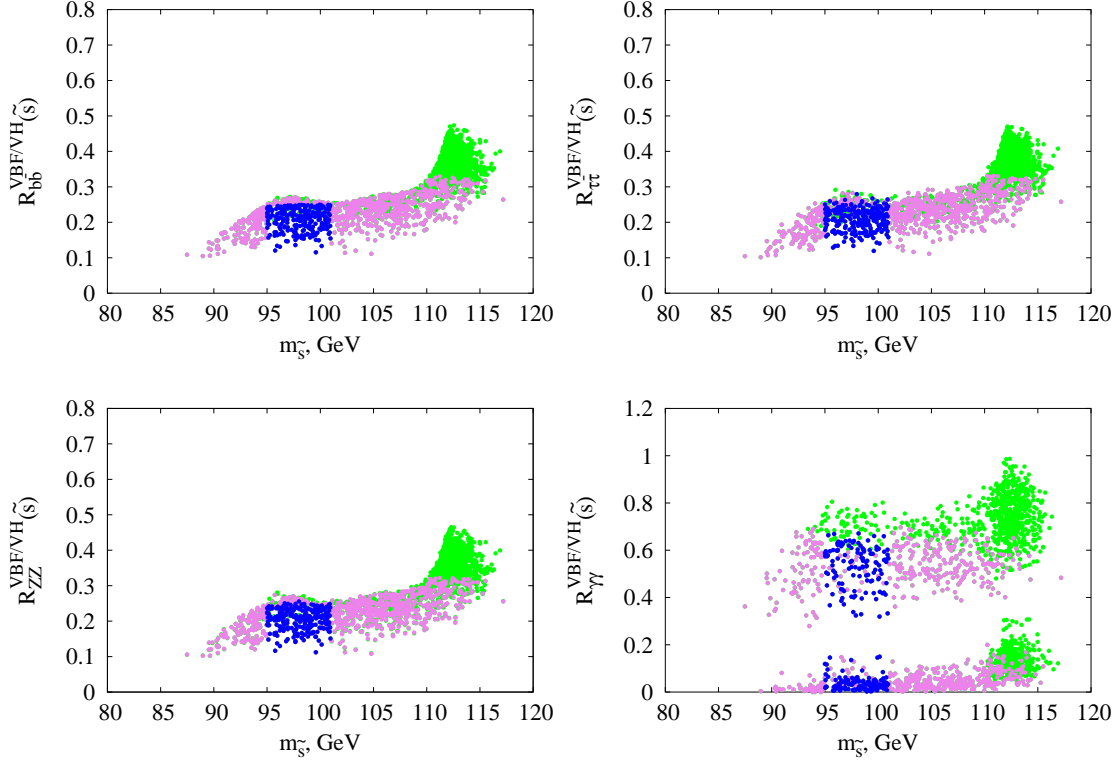


Figure 13: Scatter plots in $m_{\tilde{s}} - R_{bb}^{VBF/VH}(\tilde{s})$ (upper left panel), $m_{\tilde{s}} - R_{\tau\tau}^{VBF/VH}(\tilde{s})$ (upper right panel), $m_{\tilde{s}} - R_{WW}^{VBF/VH}(\tilde{s})$ (lower left panel), $m_{\tilde{s}} - R_{\gamma\gamma}^{VBF/VH}(\tilde{s})$ (lower right panel) planes for *Set 1*. The color notations are the same as in Fig. 4.

\tilde{h} can result in an additional increase of mass of the latter. As an attractive feature of this scenario, we have found that new sgoldstino-like scalar state \tilde{s} which is somewhat lighter than the Higgs-like boson is present in low energy spectrum. In particular, there is a region in the parameter space of the model where this state can explain 2σ LEP excess in $e^+e^- \rightarrow Z\tilde{s}$ with $\tilde{s} \rightarrow b\bar{b}$ having mass around 98 GeV.

Performing a scan over parameters for $\sqrt{F} = 10$ TeV and selecting phenomenologically acceptable models we have found that the mixing with sgoldstino results in a distinctive features in signal strengths for the Higgs-like resonance in this scenario. In gluon-gluon fusion the signal strengths for fermion and massive vector boson channels are somewhat larger than unity with values about $1.0 - 1.5$. On the contrary, for vector boson fusion or associative production with massive vector boson the signal strengths are predicted to be within the range about $0.7 - 1.0$. If sgoldstino is required to be 98 GeV LEP resonance then even more strict bounds on the signal strength are predicted, which hopefully can be probed

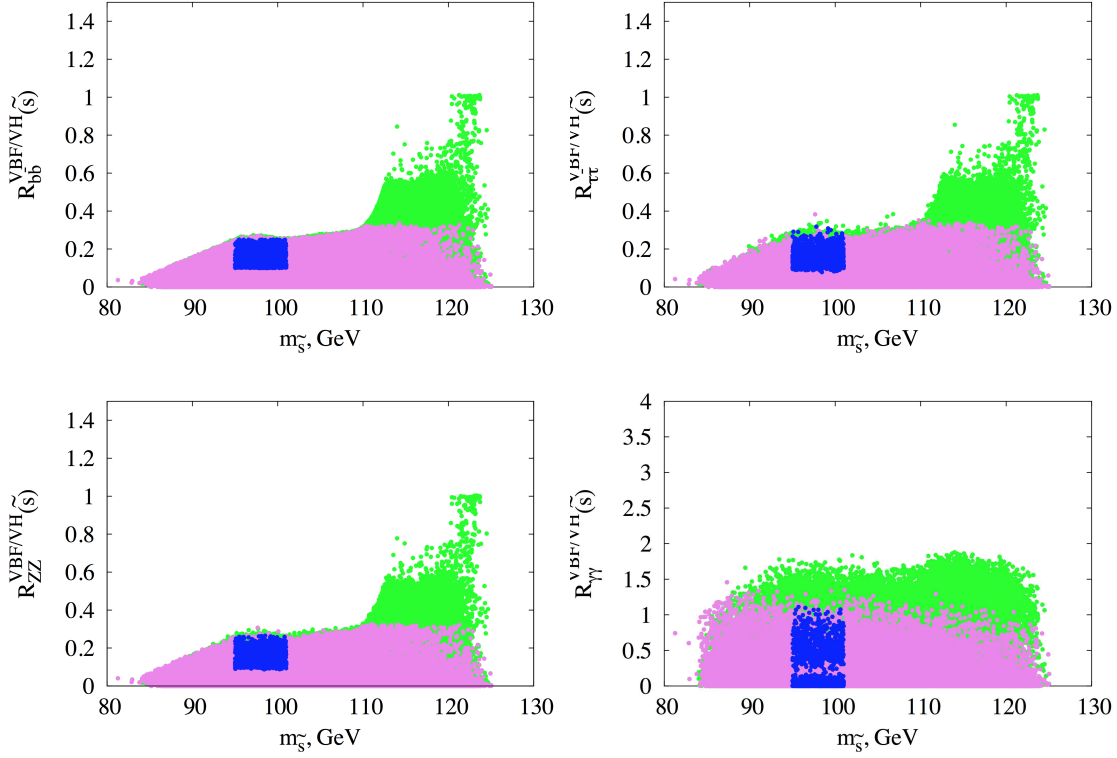


Figure 14: Scatter plots in $m_{\tilde{s}} - R_{bb}^{VBF/VH}(\tilde{s})$ (upper left panel), $m_{\tilde{s}} - R_{\tau\tau}^{VBF/VH}(\tilde{s})$ (upper right panel), $m_{\tilde{s}} - R_{WW}^{VBF/VH}(\tilde{s})$ (lower left panel), $m_{\tilde{s}} - R_{\gamma\gamma}^{VBF/VH}(\tilde{s})$ (lower right panel) planes for *Set 2*. The color notations are the same as in Fig. 4.

in the next runs of the LHC experiments.

Note that here we have performed a simplified analysis by limiting ourselves to the case of MSSM decoupling limit, zero vacuum expectation value for sgoldstino field and fixed value for supersymmetry breaking scale $\sqrt{F} = 10$ TeV. By going beyond these assumptions one could obtain that the life with sgoldstino-Higgs mixing can become even more complicated. In particular, we expect different mixing patterns due to presence of heavier Higgs boson in spectrum (see e.g. [84]) and shifts in the Yukawa couplings of the lightest Higgs boson to fermions [47]. Among the other possible phenomenological issues which are not covered in the present study we mention possibility of new decays of the lightest Higgs boson in which sgoldstino can be involved including those with flavour violation (see also Ref. [29]). For sufficiently light sgoldstinos decays $\tilde{h} \rightarrow \tilde{s}\tilde{h}^*$ with subsequent $\tilde{s} \rightarrow \gamma\gamma$ and $\tilde{h} \rightarrow b\bar{b}$ or $\tilde{h} \rightarrow \tilde{s}\tilde{s}^*$ with $\tilde{s} \rightarrow \gamma\gamma$ become possible resulting in new signatures in the Higgs boson decays. Another interesting area to explore is models of low-scale supersymmetry breaking in which gauginos

have Dirac masses (see, e.g. [85] and references therein). In this case sgoldstino interactions with the SM fields can be different as compared to the case discussed in our paper resulting in different mixing properties and the couplings of mass states. We leave investigations of these interesting possibilities for future work.

Acknowledgments We thank D. Gorbunov for valuable discussions and careful reading the manuscript. The work was supported by the RSCF grant 14-22-00161. The numerical part of the work was performed on Computational Cluster of the Theory Division of INR RAS.

A Modifications of decays $\tilde{h} \rightarrow ZZ$ and $\tilde{h} \rightarrow W^+W^-$.

In this Appendix we present formulas for partial widths of the decay of the Higgs-like resonance \tilde{h} into pair of massive vector bosons V , where V is W or Z -boson. A complication arises due to the fact that the Higgs boson h and scalar sgoldstino s have different interactions with W^\pm and Z -bosons, see Eqs. (2.30) and (2.31). Using results of Ref. [73] we obtain

$$\Gamma(\tilde{h} \rightarrow VV^*) = \delta_V \frac{G_F m_{\tilde{h}}^3}{16\pi^2 \sqrt{2}} \int d(\Delta^2) \sqrt{\lambda(m_V^2, \Delta^2, m_{\tilde{h}}^2)} \frac{\Gamma_V m_V}{|D(\Delta^2)|^2} \times \quad (\text{A.1})$$

$$\times \left[\lambda(m_V^2, \Delta^2, m_{\tilde{h}}^2) + 12 \frac{m_V^2 \Delta^2}{m_{\tilde{h}}^4} + X(\Delta) \right]$$

where

$$\lambda(x, y, z) = \left(1 - \frac{x}{z} - \frac{y}{z}\right)^2 - 4 \frac{xy}{z^2}, \quad D(\Delta^2) = \Delta^2 - m_V^2 + im_V \Gamma_V \quad (\text{A.2})$$

and

$$X(\Delta) = \frac{m_V^2 \Delta^2 f}{m_{\tilde{h}}^4} \left(12(-\Delta^2 - m_V^2 + m_{\tilde{h}}^2) + \right. \quad (\text{A.3})$$

$$\left. + 4f \left[\frac{1}{2} \Delta^4 + \frac{1}{2} (m_V^2 - m_{\tilde{h}}^2)^2 + (m_V^2 - m_{\tilde{h}}^2) \Delta^2 + \Delta^2 m_V^2 \right] \right)$$

$\delta_V = 2(1)$ for $V = W(Z)$, Δ —is 4-momenta of off-shell particle V^* and f is defined by

$$f = \frac{-M_{ZZ(2)} v}{2F m_V^2}. \quad (\text{A.4})$$

References

- [1] G. Aad *et al.* [ATLAS Collaboration], Phys. Lett. B **716** (2012) 1 [arXiv:1207.7214 [hep-ex]],
- [2] S. Chatrchyan *et al.* [CMS Collaboration], Phys. Lett. B **716** (2012) 30 [arXiv:1207.7235 [hep-ex]].
- [3] M. Spira, Fortsch. Phys. **46**, 203 (1998) [hep-ph/9705337].
- [4] A. Djouadi, Phys. Rept. **457** (2008) 1 [hep-ph/0503172].
- [5] H. E. Haber and G. L. Kane, Phys. Rept. **117** (1985) 75.
- [6] S. P. Martin, In *Kane, G.L. (ed.): Perspectives on supersymmetry II* 1-153 [hep-ph/9709356].
- [7] M. Papucci, J. T. Ruderman and A. Weiler, JHEP **1209**, 035 (2012) [arXiv:1110.6926 [hep-ph]].
- [8] L. J. Hall, D. Pinner and J. T. Ruderman, JHEP **1204**, 131 (2012) [arXiv:1112.2703 [hep-ph]].
- [9] C. Brust, A. Katz, S. Lawrence and R. Sundrum, JHEP **1203** (2012) 103 [arXiv:1110.6670 [hep-ph]].
- [10] P. Draper, P. Meade, M. Reece and D. Shih, Phys. Rev. D **85** (2012) 095007 [arXiv:1112.3068 [hep-ph]].
- [11] H. Baer, V. Barger, P. Huang and X. Tata, JHEP **1205** (2012) 109 [arXiv:1203.5539 [hep-ph]].
- [12] Z. Kang, J. Li and T. Li, JHEP **1211** (2012) 024 [arXiv:1201.5305 [hep-ph]].
- [13] K. Kowalska and E. M. Sessolo, Phys. Rev. D **88** (2013) 7, 075001 [arXiv:1307.5790 [hep-ph]].
- [14] E. Hardy, JHEP **1310** (2013) 133 [arXiv:1306.1534 [hep-ph]].
- [15] H. Baer, V. Barger, P. Huang, D. Mickelson, A. Mustafayev and X. Tata, “Naturalness, Supersymmetry and Light Higgsinos: A Snowmass Whitepaper,” arXiv:1306.2926 [hep-ph].

- [16] H. P. Nilles, Phys. Rept. **110** (1984) 1.
- [17] D. V. Volkov and V. P. Akulov, JETP Lett. **16** (1972) 438 [Pisma Zh. Eksp. Teor. Fiz. **16** (1972) 621], D. V. Volkov and V. P. Akulov, Phys. Lett. B **46** (1973) 109.
- [18] E. Cremmer, B. Julia, J. Scherk, P. van Nieuwenhuizen, S. Ferrara and L. Girardello, Phys. Lett. B **79** (1978) 231.
- [19] G. F. Giudice and R. Rattazzi, Phys. Rept. **322** (1999) 419 [hep-ph/9801271], S. L. Dubovsky, D. S. Gorbunov and S. V. Troitsky, Phys. Usp. **42** (1999) 623 [Usp. Fiz. Nauk **169** (1999) 705] [hep-ph/9905466].
- [20] J. R. Ellis, K. Enqvist and D. V. Nanopoulos, Phys. Lett. B **147** (1984) 99, J. R. Ellis, K. Enqvist and D. V. Nanopoulos, Phys. Lett. B **151** (1985) 357.
- [21] T. Gherghetta and A. Pomarol, Nucl. Phys. B **586** (2000) 141 [hep-ph/0003129].
T. Gherghetta and A. Pomarol, Nucl. Phys. B **602** (2001) 3 [hep-ph/0012378].
- [22] D. A. Dicus, S. Nandi and J. Woodside, Phys. Rev. D **41** (1990) 2347.
- [23] S. Shirai and T. T. Yanagida, Phys. Lett. B **680** (2009) 351 [arXiv:0905.4034 [hep-ph]].
- [24] K. Mawatari and B. Oehl, Eur. Phys. J. C **74** (2014) 2909 [arXiv:1402.3223 [hep-ph]].
- [25] J. R. Ellis, J. L. Lopez and D. V. Nanopoulos, Phys. Lett. B **394** (1997) 354 [hep-ph/9610470].
- [26] M. Klasen and G. Pignol, Phys. Rev. D **75** (2007) 115003 [hep-ph/0610160].
- [27] A. Brignole, F. Feruglio, M. L. Mangano and F. Zwirner, Nucl. Phys. B **526** (1998) 136 [Erratum-ibid. B **582** (2000) 759] [hep-ph/9801329].
- [28] A. Brignole, F. Feruglio and F. Zwirner, Nucl. Phys. B **516** (1998) 13 [Erratum-ibid. B **555** (1999) 653] [hep-ph/9711516].
- [29] C. Petersson, A. Romagnoni and R. Torre, JHEP **1210** (2012) 016 [arXiv:1203.4563 [hep-ph]].
- [30] M. A. Luty and E. Ponton, Phys. Rev. D **57** (1998) 4167 [hep-ph/9706268].
- [31] D. Gorbunov, V. Ilyin and B. Mele, Phys. Lett. B **502** (2001) 181 [hep-ph/0012150],

- [32] A. Djouadi and M. Drees, Phys. Lett. B **407** (1997) 243 [hep-ph/9703452].
- [33] D. A. Dicus, S. Nandi and J. Woodside, Phys. Rev. D **43** (1991) 2951.
- [34] A. Brignole and A. Rossi, Nucl. Phys. B **587** (2000) 3 [hep-ph/0006036].
- [35] D. S. Gorbunov, Nucl. Phys. B **602** (2001) 213 [hep-ph/0007325],
- [36] D. S. Gorbunov and V. A. Rubakov, Phys. Rev. D **64** (2001) 054008 [hep-ph/0012033],
- [37] D. S. Gorbunov and V. A. Rubakov, Phys. Rev. D **73** (2006) 035002 [hep-ph/0509147],
- [38] S. V. Demidov and D. S. Gorbunov, JETP Lett. **84** (2007) 479 [hep-ph/0610066],
- [39] S. V. Demidov and D. S. Gorbunov, Phys. Rev. D **85** (2012) 077701 [arXiv:1112.5230 [hep-ph]],
- [40] E. Perazzi, G. Ridolfi and F. Zwirner, Nucl. Phys. B **574** (2000) 3 [hep-ph/0001025],
- [41] E. Perazzi, G. Ridolfi and F. Zwirner, Nucl. Phys. B **590** (2000) 287 [hep-ph/0005076],
- [42] D. S. Gorbunov and N. V. Krasnikov, JHEP **0207** (2002) 043 [hep-ph/0203078],
- [43] S. V. Demidov and D. S. Gorbunov, Phys. Atom. Nucl. **69** (2006) 712 [hep-ph/0405213],
- [44] I. Antoniadis, E. Dudas, D. M. Ghilencea and P. Tziveloglou, Nucl. Phys. B **841** (2010) 157 [arXiv:1006.1662 [hep-ph]].
- [45] C. Petersson and A. Romagnoni, JHEP **1202** (2012) 142 [arXiv:1111.3368 [hep-ph]].
- [46] I. Antoniadis and D. M. Ghilencea, Nucl. Phys. B **870** (2013) 278 [arXiv:1210.8336 [hep-th]].
- [47] E. Dudas, C. Petersson and P. Tziveloglou, Nucl. Phys. B **870** (2013) 353 [arXiv:1211.5609 [hep-ph]].
- [48] I. Antoniadis, E. M. Babalic and D. M. Ghilencea, Eur. Phys. J. C **74** (2014) 9, 3050 [arXiv:1405.4314 [hep-ph]].
- [49] E. Dudas, C. Petersson and R. Torre, “Collider signatures of low scale supersymmetry breaking: A Snowmass 2013 White Paper,” arXiv:1309.1179 [hep-ph].

- [50] B. Bellazzini, C. Petersson and R. Torre, Phys. Rev. D **86** (2012) 033016 [arXiv:1207.0803 [hep-ph]].
- [51] C. Petersson, A. Romagnoni and R. Torre, Phys. Rev. D **87** (2013) 013008 [arXiv:1211.2114 [hep-ph]].
- [52] S. Demidov and K. O. Astapov, PoS QFTHEP **2013** (2013) 090.
- [53] G. F. Giudice, R. Rattazzi and J. D. Wells, Nucl. Phys. B **595** (2001) 250 [hep-ph/0002178].
- [54] R. Barate *et al.* [LEP Working Group for Higgs boson searches and ALEPH and DELPHI and L3 and OPAL Collaborations], Phys. Lett. B **565** (2003) 61 [hep-ex/0306033].
- [55] A. Brignole, F. Feruglio and F. Zwirner, Nucl. Phys. B **501** (1997) 332 [hep-ph/9703286],
- [56] A. Brignole, J. A. Casas, J. R. Espinosa and I. Navarro, Nucl. Phys. B **666** (2003) 105 [hep-ph/0301121].
- [57] D. S. Gorbunov and A. V. Semenov, “CompHEP package with light gravitino and sgoldstinos,” hep-ph/0111291.
- [58] U. Ellwanger, J. F. Gunion and C. Hugonie, JHEP **0502** (2005) 066 [hep-ph/0406215], U. Ellwanger and C. Hugonie, Comput. Phys. Commun. **175** (2006) 290 [hep-ph/0508022], G. Belanger, F. Boudjema, C. Hugonie, A. Pukhov and A. Semenov, JCAP **0509** (2005) 001 [hep-ph/0505142].
- [59] N. Chen, D. Feldman, Z. Liu and P. Nath, Phys. Lett. B **685**, 174 (2010) [arXiv:0911.0217 [hep-ph]].
- [60] Y. Kats, P. Meade, M. Reece and D. Shih, JHEP **1202** (2012) 115 [arXiv:1110.6444 [hep-ph]].
- [61] I. Melzer-Pellmann and P. Pralavorio, Eur. Phys. J. C **74** (2014) 2801 [arXiv:1404.7191 [hep-ex]].
- [62] G. D. Kribs, A. Martin and T. S. Roy, JHEP **0901**, 023 (2009) [arXiv:0807.4936 [hep-ph]].
- [63] J. T. Ruderman and D. Shih, JHEP **1208** (2012) 159 [arXiv:1103.6083 [hep-ph]].

- [64] ATLAS collaboration, “Search for Diphoton Events with Large Missing Transverse Momentum in 8 TeV pp Collision Data with the ATLAS Detector,” ATLAS-CONF-2014-001, ATLAS-COM-CONF-2013-128.
- [65] CMS Collaboration, “Search for supersymmetry in events with one photon, jets and missing transverse energy at $\sqrt{s} = 8$ TeV,” CMS-PAS-SUS-14-004.
- [66] CMS Collaboration, “Search for supersymmetry in two-photons+jet events with razor variables in pp collisions at $\sqrt{s} = 8$ TeV,” CMS-PAS-SUS-14-008.
- [67] V. Khachatryan *et al.* [CMS Collaboration], “Searches for electroweak neutralino and chargino production in channels with Higgs, Z, and W bosons in pp collisions at 8 TeV,” arXiv:1409.3168 [hep-ex].
- [68] V. Khachatryan *et al.* [CMS Collaboration], Eur. Phys. J. C **74** (2014) 9, 3036 [arXiv:1405.7570 [hep-ex]].
- [69] S. Chatrchyan *et al.* [CMS Collaboration], Phys. Rev. D **90**, 032006 (2014) [arXiv:1404.5801 [hep-ex]].
- [70] CMS Collaboration, CMS-PAS-SUS-13-008.
- [71] CMS Collaboration, CMS-PAS-SUS-13-019.
- [72] CMS Collaboration, CMS-PAS-SUS-14-011.
- [73] J. C. Romao and S. Andringa, Eur. Phys. J. C **7** (1999) 631 [hep-ph/9807536].
- [74] S. Schael *et al.* [ALEPH and DELPHI and L3 and OPAL and LEP Working Group for Higgs Boson Searches Collaborations], Eur. Phys. J. C **47**, 547 (2006) [hep-ex/0602042].
- [75] V. M. Abazov *et al.* [D0 Collaboration], Phys. Rev. D **88**, no. 5, 052011 (2013) [arXiv:1303.0823 [hep-ex]].
- [76] LEP Higgs Working Group for Higgs boson searches Collaboration, “Searches for Higgs Bosons Decaying into Photons: Combined Results from the LEP Experiments”, LHWG Note/2002-02
- [77] G. Belanger, U. Ellwanger, J. F. Gunion, Y. Jiang, S. Kraml and J. H. Schwarz, JHEP **1301**, 069 (2013) [arXiv:1210.1976 [hep-ph]].

- [78] B. Bhattacharjee, M. Chakraborti, A. Chakraborty, U. Chattopadhyay, D. Das and D. K. Ghosh, Phys. Rev. D **88**, no. 3, 035011 (2013) [arXiv:1305.4020 [hep-ph]].
- [79] P. Abreu *et al.* [DELPHI Collaboration], Phys. Lett. B **494** (2000) 203 [hep-ex/0102044].
- [80] P. de Aquino, F. Maltoni, K. Mawatari and B. Oehl, JHEP **1210** (2012) 008 [arXiv:1206.7098 [hep-ph]].
- [81] S. Chatrchyan *et al.* [CMS Collaboration], JHEP **1401**, 096 (2014) [arXiv:1312.1129 [hep-ex]], S. Chatrchyan *et al.* [CMS Collaboration], Phys. Rev. D **89**, 092007 (2014) [arXiv:1312.5353 [hep-ex]], S. Chatrchyan *et al.* [CMS Collaboration], JHEP **1405**, 104 (2014) [arXiv:1401.5041 [hep-ex]], S. Chatrchyan *et al.* [CMS Collaboration], Phys. Rev. D **89**, no. 1, 012003 (2014) [arXiv:1310.3687 [hep-ex]], G. Aad *et al.* [ATLAS Collaboration], Phys. Lett. B **726** (2013) 88 [Erratum-ibid. B **734** (2014) 406] [arXiv:1307.1427 [hep-ex]], G. Aad *et al.* [ATLAS Collaboration], Phys. Rev. D **90** (2014) 052004 [arXiv:1406.3827 [hep-ex]], ATLAS-CONF-2014-060, ATLAS-CONF-2014-009, ATLAS-CONF-2014-061
- [82] [CMS Collaboration], CMS-PAS-HIG-13-001.
- [83] [ATLAS Collaboration], ATLAS-CONF-2012-168, ATLAS-COM-CONF-2012-203.
- [84] T. Han, T. Li, S. Su and L. T. Wang, JHEP **1311** (2013) 053 [arXiv:1306.3229 [hep-ph]].
- [85] M. D. Goodsell and P. Tziveloglou, Nucl. Phys. B **889** (2014) 650 [arXiv:1407.5076 [hep-ph]].